MODELLING AND SIMULATION OF UNSTEADY STATE HEAT AND

MASS TRANSFER IN THE ROASTING OF MEAT

by

NEERA SINGH

B. Tech., Indian Institute of Technology,

Kanpur, 1981

A MASTER'S REPORT

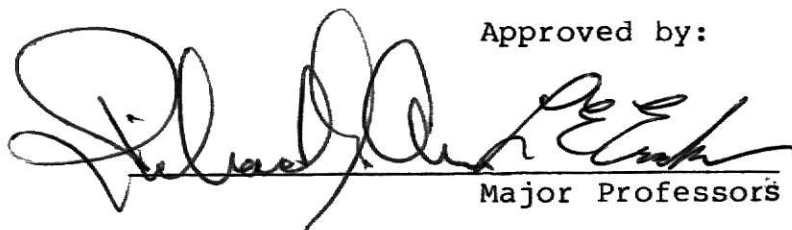submitted in partial fulfillment of the

requirement for the degree

MASTER OF SCIENCE

Department of Chemical Engineering

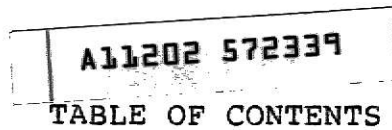KANSAS STATE UNIVERSITY

Manhattan, Kansas

1983

Approved by:

Major Professors

TABLE OF CONTENTS

ILLEGIBLE DOCUMENT

THE FOLLOWING
DOCUMENT(S) IS OF
POOR LEGIBILITY IN
THE ORIGINAL

THIS IS THE BEST
COPY AVAILABLE

P-474

THIS BOOK CONTAINS NUMEROUS PAGES WITH DIAGRAMS THAT ARE CROOKED COMPARED TO THE REST OF THE INFORMATION ON THE PAGE.

THIS IS AS RECEIVED FROM CUSTOMER.

LIST OF TABLES

LIST OF FIGURES

List of Figures (cont.)

FIGURES   Page

List of Figures (cont.)

I. INTRODUCTION

Problem Relevance

Considerable energy is used to store and prepare meat. Reduction of energy consumption can be accomplished in the industrial preparation of meat by optimization of meat cooking procedures. To achieve this, a thorough understanding of heat and mass transfer during the cooking process is essential so that energy supplied to raise the internal temperature of the meat may be utilized economically. In the cooking of meat, heat is supplied to improve the tenderness and flavor and also to destroy microorganisms. During the heating process, water retained in proteins is released and it is then transported to the surface through a complex network of fibers and muscles. Water is evaporated from the surface into the hot air. Therefore, understanding the process of meat cooking involves characterization of unsteady state, simultaneous, heat and mass transfer in a complex porous system.

Background and Previous Work

During the roasting of meat, there is an exchange of heat and mass (water) between the air and the product. Heat is transferred from the air to the meat and moisture is evaporated from the meat. This process results in three distinct stages of drying. The first stage is a constant drying rate period which is followed by two falling rate periods as shown in Figure 1.1.
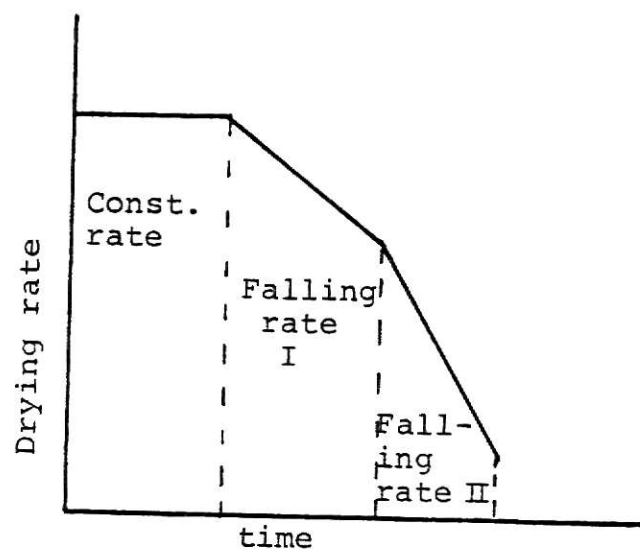
Fig. 1.1 Drying rate curve

In the constant drying rate period, the rate of moisture
loss is constant and is independent of the amount of moisture
present in the meat. The moisture is transported from
within at a faster rate or at the same rate as water is
evaporated from the surface. For low Biot number (Biot no. =
hd/k), the water in the meat can be assumed to be free water
and hence evaporation at the solid surface can be thought of
as water evaporating from a shallow container [1].

The falling rate period starts when the surface tempera-
ture begins to rise above the wet bulb temperature. In this
stage, the migration of moisture to the surface slows down
considerably, so, at any point, there is not sufficient water
on the surface to evaporate at the same rate as the constant
rate period. The surface is much drier and the evaporating zone
moves into the solid. In the roasting of meat, this results in
the formation of crust and the evaporation occurs in the vicinity
of the 100°C isotherm. The transport of water below 100°C

is similar to capillary liquid flow. The transport of moisture in the crust can be assumed to be in vapor phase [4]. In the falling rate period, the unbounded moisture (or free water) assumption in the meat can no longer be applied.

Considerable research in the roasting of meat has already been reported in the literature. The work most closely related to this work is that of Godsalve et al. [2,3], Bengtsson, [6], Skjolderbrand [4,5] and Bimbenet et al. [7]. These workers have studied the heat and mass transfer in meat during roasting. Godsalve et al. [2] presented experimental data for water emission rates from the surface of beef muscle that was heated in a dry atmosphere. Air flow rate, temperature, and humidity were continuously controlled at all times. From the data, a qualitative model of heat and mass transfer during the roasting process was deduced. In a later paper [3], they examined the effect of air flow rate, orientation of the muscle fibers, and post mortem treatment of the muscle being cooked. They concluded that the variation in flow rate did not change the basic mechanism of water transport, but it did change the water emission rate in the constant and falling rate periods. Perpendicular fiber orientation with respect to air flow rate gave a higher rate of water loss in the early stages of cooking.

Skjoldebrand et al. [4] presented a theory of how the water content inside the crust depends on the time temperature history of different meat recipes. It was shown that moisture within the crust was very low, but it increased markedly near the

evaporating zone.   A model was also developed for calculating the water content profile and thermal conductivity in the crust. The same authors [5] also qualitatively analyzed the heat and mass transfer between air and the product in a forced convection oven. Bengtsson et al. [6] presented experimental data to assess the weight loss and distribution of temperature and moisture in beef samples as a function of initial and ambient temperature. The authors only considered the constant drying rate period and also provided some simulated temperature profiles. No mathematical model was explicitly provided in the paper. Bimbenet et al. [7] studied heat and mass transfer during drying of a semi-infinite solid in warm air. A mathematical model which gives an exact solution was provided for the one dimensional case. The model was valid only for the constant drying rate period.

Work done by Hamm [15], Hung et al. [18] and Godsalve et al. [2] indicated that water is expelled from the beef muscle because of protein denaturation. Heat of denaturation of meat and the resulting release of juices are factors that should be of importance to heat and mass transfer during cooking. This effect has been considered by Hamm and Deatherage [19] and Laakonen [20]. The effect of water holding capacity of the muscle has been discussed by Hamm [15] and Bouton et al. [16,17]. Funk and Boyle [22] found that cooking rate increased as fat content or oven temperature was increased. Drip losses were not significantly affected by oven temperature, but they increased with increased fat content.

The thermal conductivity of beef has been measured

previously by Okos et al. [9], Hill et al. [8] and Woodams et al. [12]. Hill et al. [8] and Lentz [13] reported that the thermal conductivity of frozen meat is greater for heat flow parallel to the muscle than for heat flow perpendicular to fiber. Stuart and Closset [14] showed that fiber structure has an important influence on heat and mass transfer in freeze dried beef. A compilation of thermal properties of beef was given by Polley, Snyder and Kotnour [10]. The heat transfer coefficient at the surface of meat can be estimated from available correlations [23].

The use of microwave cooking has been investigated by Moore et al. [24], Voris and Duyne [25] and Korschgen and Baldwin [26]. Moore et al. indicated that dry roasting in a conventional oven resulted in less loss of juice and more even roasting as compared with microwave roasting. Contrary to these findings, Korschgen and Baldwin [26] reported that there was no significant difference in cooking loss by the two different techniques. They also noted very little differ- ence in flavor and juiciness for microwave and conventional roasting. Voris and Duyne [25] came to the same conclusions. Energy requirement associated with microwave cooking has been found to be considerably less than that for conventional roasting [25,26]. No work was found where microwave roasting was carried out at controlled conditions of temperature and humidity.

Numerical Solution for Partial Differential Equations

Parabolic partial differential equations arise from unsteady state problems in which transport by conduction or diffusion is important. The general form of parabolic partial differential equation in one dimension is

$$\frac{\partial^2 u}{\partial x^2} = \frac{\partial u}{\partial t} \tag{1.1}$$

Following are the boundary conditions which may exist.

1)   At time t = 0, u = 0 for all values of x.

   For time t > 0, u = 1 at x = 0

   For time t > 0, u = 0 at x = 1

2)   At time t = 0, u = 0 for all values of x

   For time t > 0, $\frac{du}{dx}$ + hu + const. = 0 at x = 1

                    (convection BC)

   For time t > 0, $\frac{du}{dx}$ = 0 at x = 0

The length variable in equation (1.1) varies from 0 to 1 and the time variable t can take any value on the positive t axis. The region represented by the two independent variables, x and t, is a part of the x-t plane as shown in Figure 1.2.

For numerical computations, the continuous variables x and t are replaced by discrete variables defined by points on the shaded plane as shown in Figure 1.2. The grid points are **spaced** so that they are ∆x apart in the x direction and ∆t apart in the t direction.

Fig. 1.2. Two dimensional grid

The index i is used to indicate position on the x axis and
k to indicate the position on the t axis. The dependent
variable u is a function of the two independent variables
x and t.

A number of finite difference equations analogous to
equation (1.1) can be written to solve the partial differen-
tial equation numerically. The forward or the explicit
difference equation is the simplest to formulate (though it
is inefficient to use). In the forward difference equation, th
finite diff. analog of $(\partial^2 u/\partial x^2)$ is written for the known
time level t_k.

$$\therefore \left(\frac{\partial^2 u}{\partial x^2}\right)_i = \frac{u_{i+1,k} - 2u_{i,k} + u_{i-1,k}}{(\Delta x)^2} \tag{1.2}$$

$$\text{and} \quad \left(\frac{\partial u}{\partial t}\right) = \frac{u_{i,k+1} - u_{i,k}}{\Delta t} \tag{1.3}$$

Hence, $u_{i,k+1} = \frac{\Delta t}{(\Delta x)^2} \left[u_{i+1,k} + u_{i-1,k} \right] + \left[1 - \frac{2\Delta t}{(\Delta x)^2} \right] u_{i,k}$ (1.4)

In this scheme, the value of the dependent variable u can be calculated directly from equation 1.4. This method is the simplest to use but it is very inefficient. For the numerical solution to converge, a very stringent condition between the time interval, Δt, and the length interval, Δx, must be satisfied. This condition requires the ratio $\Delta t/(\Delta x)^2$ to be less than 1/2 [21]. If this condition is not met, the coefficient of $u_{i,k}$ in equation (1.4) will become negative and this will cause the value of u_i to oscillate from one time step to the next. This restriction is a rather serious one. To avoid truncation errors in the x direction, Δx has to be kept small and, for the solution to be stable, Δt should be of the same order of magnitude as $(\Delta x)^2$. As a result, small values of the time increment Δt must be used even though larger values could have been used without causing truncation errors in the t direction.

The backward difference equation does not have any such restriction on the size of Δt for stability. In this method, the analog of $(\partial^2 u/\partial x^2)$ is written for the next (unknown) time level t_{k+1}.

$$\left(\frac{\partial^2 u}{\partial x^2} \right)_i = \frac{u_{i+1,k+1} - 2u_{i,k+1} + u_{i-1,k+1}}{(\Delta x)^2}$$ (1.5)

$$\left(\frac{\partial u}{\partial t}\right)_i = \frac{u_{i,k+1} - u_{i,k}}{(\Delta t)} \tag{1.6}$$

$$\therefore \quad \frac{u_{i+1,k+1} - 2u_{i,k+1} + u_{i-1,k+1}}{(\Delta x)^2} = \frac{u_{i,k+1} - u_{i,k}}{(\Delta t)}$$

Hence $u_{i-1,k+1} + \left[-2 - \frac{(\Delta x)^2}{\Delta t}\right] u_{i,k+1} + u_{i+1,k+1} = \frac{-(\Delta x)^2}{\Delta t} u_{i,k}$

$$\tag{1.7}$$

Equation (1.7) is an implicit equation. The value of the dependent variable u_i at the next time step t_{k+1} cannot be solved directly as in the forward difference equation. Unlike equation 1.4, equation 1.7 contains three values of the dependent variable u_i at the next time level t_{k+1} (which is not known). The equation can be solved by writing the difference equation for all the grid points in the x-direction. The resulting set of equations results in a tridiagonal matrix which can be solved simultaneously by applying the appropriate boundary conditions. Stability analysis shows that there is no restriction on the size of Δt, and it can be fixed independent of the size of Δx. Both the backward and the forward difference equations are first order correct in time.

The Crank and Nicholson Method [27] for solving the parabolic partial differential equation is second order correct in time and it also does not have any restriction on the size of Δt. In this method, all finite difference analogs are written about the point x_i and $t_{k+1/2}$.

$$\left(\frac{\partial u}{\partial t}\right)_{i,k+1/2} = \frac{u_{i,k+1} - u_{ik}}{\Delta t} \tag{1.8}$$

In approximating the derivative $(\partial^2 u/\partial x^2)_{i,k+1/2}$, an arithmatic average of its finite difference analog at point x_i, t_k and x_i, t_{k+1} is taken. So basically it is an average of the forward and backward and difference equations.

$$\left(\frac{\partial^2 u}{\partial x^2}\right)_{i,k+\frac{1}{2}} = \frac{1}{2}\left[\frac{u_{i+1,k} - 2u_{i,k} + u_{i-1,k}}{(\Delta x)^2} + \frac{u_{i+1,k+1} - 2u_{i,k+1} + u_{i-1,k+1}}{(\Delta x)^2}\right] \tag{1.9}$$

On combining equation (1.8) and 1.9) we get

$$u_{i-1,k+1} + \left[-2 - \frac{2(\Delta x)^2}{\Delta t}\right] u_{i,k+1} + u_{i+1,k+1} =$$

$$-u_{i-1,k} + \left[2 - \frac{2(\Delta x)^2}{\Delta t}\right] u_{i,k} - u_{i+1,k} \tag{1.10}$$

Equation 1.10, like the backward difference equation is an implicit equation, but unlike the backward difference equation it is second order correct in time. The Crank and Nicholson equation requires more computations per single time step than the backward difference equation, but since it is second order correct in time, larger values of Δt can be used without causing serious truncation errors.

The backward difference equation can be used satisfactorily for both kinds of boundary conditions discussed earlier. The Crank and Nicholson equation works good for the first

boundary condition. However, when the convection boundary condition is applied, the value of u oscillates at the boundary for large values of the heat transfer coefficient (h). Therefore, for large values of h, the Crank and Nicholson equation can no longer be used to solve the partial differential equation numerically [21].

Heat conduction or diffusion in two or three space dimensions can also be described by the parabolic partial differential equation and it has the following form.

In two space dimensions
$$\frac{\partial^2 u}{\partial x^2} + \frac{\partial^2 u}{\partial y^2} = \frac{\partial u}{\partial t} \tag{1.11}$$

In three space dimensions
$$\frac{\partial^2 u}{\partial x^2} + \frac{\partial^2 u}{\partial y^2} + \frac{\partial^2 u}{\partial z^2} = \frac{\partial u}{\partial t} \tag{1.12}$$

where x, y and z are three space dimensions.

It has been shown that the Crank and Nicholson method for solving multidimensional parabolic differential equations is impractical [21]. The forward difference or the explicit method of solution has very stringent requirements for the time increment and space increments for stability. For the two dimensional case, the condition between Δt, Δx and Δy to be satisfied is [27]

$$\Delta t \leq \frac{1}{2[(\Delta x)^{-2} + (\Delta y)^{-2}]}$$

This restriction (as discussed earlier) makes this method of solution very inefficient. The implicit method requires a large number of iterations for adequate convergence [27].

One of the most efficient schemes for solving parabolic differ-
ential equations in two or more space dimension is the "Implicit
Alternating Direction" (I.A.D.) method [21,27]. For the two dimen-
sional case, this method employs two difference equations which
are used over successive time steps of duration $\Delta t/2$. The first
equation is implicit only in the x direction and the second
equation is implicit only in the y direction. The first
equation contains analog to $\partial^2 u/\partial x^2$ written for the first time
step $t_k + \Delta t/2$ (abbreviated as *) and the analog to $(\partial^2 u/\partial y^2)$
at the time level t_k. The final equation results in this form.

$$\frac{u^*_{i+1,j} - 2u^*_{i,j} + u^*_{i-1,j}}{(\Delta x)^2} + \frac{u_{i,j+1,k} - 2u_{i,j,k} + u_{i,j-1,k}}{(\Delta y)^2}$$

$$= \frac{u^*_{i,j} - u_{i,j,k}}{\Delta t/2}$$

Let $\Delta x = \Delta y$

$$\therefore \quad -u^*_{i-1,j} + 2\left[\frac{(\Delta x)^2}{\Delta t} + 1\right] u^*_{i,j} - u^*_{i+1,j}$$

$$= u_{i,j-1,k} + 2\left[\frac{(\Delta x)^2}{\Delta t} - 1\right] u_{i,j,k} + u_{i,j+1,k}$$

$$(1.13)$$

The second equation of the I.A.D. method contains the analog
to $(\partial^2 u/\partial y^2)$ written for the time level $t_k + \Delta t = t_{k+1}$ and the
analog to $(\partial^2 u/\partial x^2)$ for the time level $t_k + \Delta t/2$.

$$\frac{u_{i,j+1,k+1}-2u_{i,j,k+1}+u_{i,j-1,k+1}}{(\Delta y)^2} + \frac{u^*_{i+1,j}-2u^*_{i,j}+u^*_{i-1,j}}{(\Delta x)^2}$$

$$= \frac{u_{i,j,k+1}-u^*_{i,j}}{\Delta t/2} \qquad (1.14)$$

Since $\Delta x = \Delta y$, we can reduce equation 1.14 to

$$-u_{i,j-1,k+1}+2[\frac{(\Delta x)^2}{\Delta t} +1]\ u_{i,j,k+1} - u_{i,j+1,k+1}$$

$$= u^*_{i-1,j}+2[\frac{(\Delta x)^2}{\Delta t} -1]u^*_{i,j}+u^*_{i+1,j} \qquad (1.15)$$

Equation 1.13 can be solved first and the value of u at the intermediate time step used to solve eq. 1.14. Both equations, 1.13 and 1.15 , when written for the grid points, are reduced to a system of equations with a tridiagonal matrix. On applying the appropriate boundary conditions, the solution is straight forward.

II. PROBLEM FORMULATION

Mathematical Modelling

In convection oven roasting of meat, there is an exchange
of heat and mass (water) between the meat and the hot air in
the oven. Heat flows into the meat thus raising its internal
temperature. During the heating process, water retained by
the proteins is released, and it migrates to the surface through
a complex porous system. A certain amount of heat (known as
heat of denaturation) is also released with the release of
juices from the proteins. The actual mechanism of transport
of water through the complex network of fibers and muscles is
not very well understood. For the sake of simplicity, the
flow of water inside the meat can be thought of as a capillary
liquid flow [4]. The water which migrates to the surface is
evaporated into the hot air in the oven, thus increasing the
oven humidity. As the internal temperature of the meat is
raised, the fat content contained in it also melts around the
fiber and may drip to the bottom of the container.

The mathematical model proposed here to describe the
unsteady state heat and mass transfer during the roasting of
meat neglects these drip losses. In addition to this, heat of
denaturation will not be considered. Only the constant rate
period of drying is considered. During this stage of drying,
the migration of water to the surface is fast enough so that

there is sufficient water at the surface to evaporate at all times. The following assumptions are made to formulate the model

1) Water at the meat surface behaves like free or unbounded water.

2) The thermal conductivity of meat remeains constant during the heating process.

3) The heat transfer coefficient between air and meat remains constant.

4) The third dimension of the meat is much larger than the other two dimensions. Therefore, heat transfer is neglected in the third direction.

5) The temperature in the oven remains constant during the entire roasting process.

All these assumptions are fairly reasonable and we do not encounter any serious problems when we incorporate them in our model. Assumption No. 1 is valid for the constant drying period and it can be applied safely when the Biot. No. (Biot No.= hd/k) is low [1].

Heat transfer within the meat can be given by Fourier's Law

$$\frac{\partial \theta}{\partial t} = \alpha [\frac{\partial^2 \theta}{\partial X^2} + \frac{\partial^2 \theta}{\partial Y^2} + \frac{\partial^2 \theta}{\partial Z^2}] \tag{2.1}$$

Since the third dimension (Z) of meat is much larger than the X and Y dimensions (Assumption No. 4), equation 2.1 can be reduced to two space dimensions.

$$\frac{\partial \theta}{\partial t} = \alpha [\frac{\partial^2 \theta}{\partial X^2} + \frac{\partial^2 \theta}{\partial Y^2}] \qquad (2.2)$$

The boundary conditions are

1) at t=0, $\theta = \theta_o$ for all values of X between 0 and a,

   and all values of Y between 0 and b.

2) (Heat from air) = (Heat absorbed in evaporating water)

   + (Heat flowing into the meat)

or $h(\theta_a - \theta) = \lambda k_p (P_s - P_a) - k (\frac{\partial \theta}{\partial X})_{X=0}$

$$-(\frac{\partial \theta}{\partial X})_{X=0} = \frac{h}{k} [\theta_a - \theta] - \frac{\lambda k_p}{k} [P_s - P_a] \qquad (2.4)$$

3) Similarly $(\frac{\partial \theta}{\partial X})_{X=a} = \frac{h}{k}[\theta_a - \theta] - \frac{\lambda k_p}{k} [P_s - P_a)$ (2.5)

Similar boundary conditions can be written for Y = 0 and Y = b.
The parameters used in the above equation are

$\alpha = \frac{k}{\rho c_p}$ = Thermal diffusivity of meat (m^2/sec)

k = Thermal conductivity of meat (J/msec^{o}C)

k_p = Mass transfer coefficient between air and meat

$$\left[\frac{kg}{m^2 Pascals\ sec} = sec/m\right]$$

θ_a = Ambient temperature, ^{o}C

λ = Latent heat of vaporization of water (J/kg)

P_a = Partial pressure of water vapor in air (Pascals)

P_s = Water Vapor Pressure at the meat surface temperature (Pascals)

For this period of drying, water at the meat surface is assumed
to be unbound (assumption No. 1). Hence P_s can be taken as

the vapor pressure of pure water at the surface temperature

$$:\cdot \quad P_s = A + B\theta \tag{2.6}$$

A linear relationship of P_s and θ is used because it is easy to apply in the tridiagonal matrix to solve the partial differential equation using the Implicit Alternating Direction (I.A.D.) method. As shown below, this approximation does not introduce any serious errors if we subdivide the entire temperature range into small increments and calculate A and B separately for each increment. In the roasting of meat, the maximum temperature of the surface is approximately $90^O C$ (during the constant drying rate period). Let us divide the temperature range ($0^O C$ - $90^O C$) into four temperature ranges.

range a	$0^O C < \theta \le 30^O C$
range b	$30^O C < \theta \le 50^O C$
range c	$50^O C < \theta \le 70^O C$
range d	$70^O C < \theta \le 90^O C$

The coefficients A and B of equation 2.6 for each of these temperature zones may be estimated using the least square method and literature data [27].

From Table 2.2, it can be seen that the maximum error introduced in the calculation of P_s is approximately 5%.

Table 2.1.   Least Square Estimates of 'A' and 'B' for the different temperature ranges

Temperature Range ($^{\circ}$C)	A (Pascals)	B Pascals/$^{\circ}$C
$0 < \theta \leq 30$	-126.35	140.85
$30 < \theta \leq 50$	-8,357.00	412.21
$50 < \theta \leq 70$	-36,001.81	958.89
$70 < \theta \leq 90$	-108,230.00	1,983.65

Table 2.2.   Comparison of P_s actual and P_s calculated

Temp ($^{\circ}$C)	P_s actual (Pascals)	P_s calculated (Pascals)	% error
10	1,249.50	1,282.15	1.6
30	4,319.08	4,099.15	5.1
50	12,563.35	12,253.50	2.4
70	31,741.13	31,120.49	2.0
90	71,414.15	70,207.62	1.5

Equations (2.2) and its boundary conditions may be written in dimensionless form by introducing the dimensionless variables:

$$y = Y/a$$

$$x = X/a$$

$$T = \frac{\theta - \theta_0}{\theta_a - \theta_0}$$

and $\tau = \alpha t/a^2$

On substituting these dimensionless variables, equation 2.2 and its boundary conditions have the following form

$$\frac{\partial^2 T}{\partial x^2} + \frac{\partial^2 T}{\partial y^2} = \frac{\partial T}{\partial \tau} \qquad (2.7)$$

at $\tau = 0$, $T = 1.0$ for all values of x between 0 and 1

and y between 0 and b/a (2.8)

$$-\left(\frac{dT}{dx}\right)_{x=0} = \frac{ah}{k}\{1-T\} - \frac{a\lambda k_p}{k}\left[\frac{\bar{A}-P_a+B\theta_O}{\theta_a-\theta_O} + BT\right] \qquad (2.9)$$

$$\left(\frac{dT}{dx}\right)_{x=1} = \frac{ah}{k}\{1-T\} - \frac{a\lambda k_p}{k}\left[\frac{\bar{A}-P_a+B\theta_O}{\theta_a-\theta_O} + BT\right] \qquad (2.10)$$

Similar dimensionless equations can be written for $y = 0$ and $y = b/a$

Equation 2.6 is a parabolic partial differential equation in two space dimensions. As discussed in the previous section, there are several schemes to solve this equation numerically. The most efficient method for solving this equation is the Implicit Alternating Direction (I.A.D.) method and this method will be used in this report.

When using a finite difference technique to solve a partial differential equation, the region of interest must be divided into a network of grid points. The dimensionless variable x varies from 0 to 1 and the variable y varies from 0 to b/a. Because of symmetry, it suffices to solve the problem
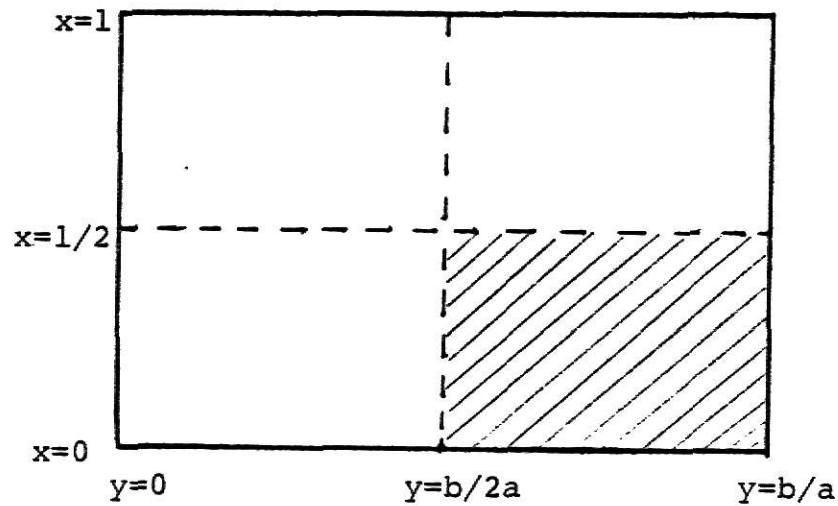
Fig. 2.1. Two dimensional heat flow
in the meat piece.

for one quadrant only (as shown in Figure 2.1). From symmetry
again, there is no heat flux across the axis $x = 1/2$ and
$y = b/2a$ and these two sides of the quadrant can be thought of
as perfectly insulated boundaries.

Consider the shaded quadrant in Figure 2.1, divided into
m and n segments (in the y and x directions) of equal length
Δx. In this way, $(m+1) \cdot (n+1)$ grid points are established in
the entire region of interest as shown in Figure 2.2 below.
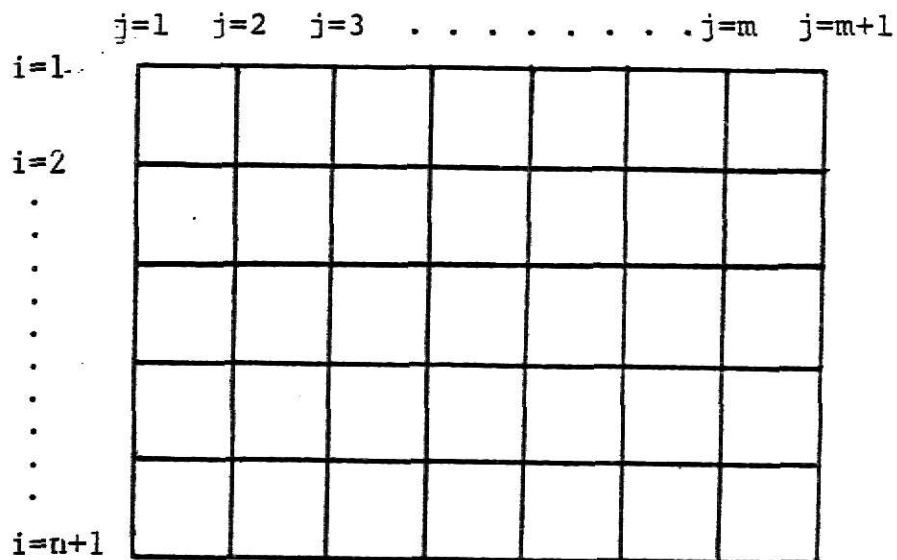
Fig. 2.2. Arrangement of grid points

Subscripts i, j and k can be used to denote the grid point (i,j) at a time level t_k (i represents position on the x axis and j represents position on the y axis). The I.A.D. method can be summarized by equations 1.13 and 1.15. Let T and T* refer to temperature at the beginning and end of the half time step $\Delta\tau/2$, respectively. Applying equation 1.13 for each grid point i = 1, 2, 3, 4...n in the jth column gives the following tridiagonal system for the jth column

$$-T^*_{0,j} + bT^*_{1,j} - T^*_{2,j} \qquad\qquad\qquad = d_1$$

$$- T^*_{1,j} + bT^*_{2,j} - T^*_{3,j} \qquad\qquad = d_2$$

$$- T^*_{2,j} + bT^*_{3,j} - T^*_{4,j} \qquad = d_3$$

$$\vdots$$

$$- T^*_{n-2,j} + bT^*_{n-1,j} - T^*_{n,j} = d_{n-1}$$

$$-T^*_{n-1,j} + bT^*_{n,j} - T^*_{n+1,j}$$

$$= d_n$$

where

$$d_i = T_{i,j-1} + fT_{i,j} + T_{i,j+1}$$

and

$$b = 2\left[\frac{(\Delta x)^2}{\Delta\tau} + 1\right]$$

$$f = 2\left[\frac{(\Delta x)^2}{\Delta\tau} - 1\right]$$

From symmetry, $T^*_{0,j} = T^*_{2,j}$. Therefore, the first equation (for i = 1) of the tridiagonal set of equations reduces to

$$bT_1^*{}_{,j} - 2T_2^*{}_{,j} = d_1$$

If $T^*_{n+1,j}$ can be written in terms of $T^*_{n,j}$ (in the nth equation), the first and the last equation will have only two unknown variables and the entire tridiagonal matrix can be solved by the algorithm given in the appendix . $T^*_{n+1,j}$ can be obtained in terms of $T^*_{n,j}$ from the convection boundary condition. Expanding the temperature at the grid point (n,j) in a Taylor series and neglecting the powers higher than second gives:

$$T^*_{n,j} = T^*_{n+1,j} + \frac{\partial T^*}{\partial x}\bigg|_{n+1,j} (-\Delta x) + \frac{\partial^2 T^*}{\partial x^2}\bigg|_{n+1,j} \frac{(-\Delta x)^2}{2}$$

$$\therefore \frac{\partial^2 T^*}{\partial x^2}\bigg|_{n+1,j} = \frac{2}{(\Delta x)^2}\left[T^*_{n,j} - \frac{\partial T^*}{\partial x}\bigg|_{n+1,j}(-\Delta x) - T^*_{n+1,j}\right] \quad (2.11)$$

$\dfrac{\partial T^*}{\partial x}\bigg|_{n+1,j}$ can be obtained from the convection B.C.

$$\frac{\partial T^*}{\partial x}\bigg|_{n+1,j} = \frac{ah}{k}[1-T^*_{n+1,j}] - \frac{a\lambda k_D}{k}\left[\frac{A-P_a+B\theta_0}{\theta_a-\theta_0} + BT^*_{n+1,j}\right]$$

On substituting $\dfrac{\partial T^*}{\partial x}\bigg|_{n+1,j}$ in equation 2.11, we get

$$\frac{\partial^2 T^*}{\partial x^2}\bigg|_{n+1,j} = \frac{2}{(\Delta x)^2}[T^*_{n,j} - T^*_{n+1,j} \{1 + \frac{ah\Delta x}{k} + \frac{a\lambda k_p \ B\Delta x}{k}\} +$$

$$\frac{ah\Delta x}{k} - \frac{a\lambda k_p \Delta x}{k} \{\frac{A - P_a + B\theta_o}{\theta_a - \theta_o}\}] \qquad (2.12)$$

The temperature at the grid point (n+1,j) must also satisfy equation 2.7. Writing the finite difference analog of $\partial^2 T/\partial y^2\big|_{n+1,j}$ at the beginning of the half time step $\Delta\tau/2$ and the finite difference analog of $\partial^2 T/\partial x^2$ at the end of the half time step $\Delta\tau/2$ gives:

$$\frac{\partial^2 T^*}{\partial x^2}\bigg|_{n+1,j} + \frac{\partial^2 T}{\partial y^2}\bigg|_{n+1,j} = \frac{T^*_{n+1,j} - T_{n+1,j}}{\Delta\tau/2}.$$

$\partial^2 T^*/\partial x^2\big|_{n+1,j}$ is given by equation 2.12

$$\frac{\partial^2 T}{\partial y^2}\bigg|_{n+1,j} = \frac{T_{n+1,j-1} - 2T_{n+1,j} + T_{n+1,j+1}}{(\Delta x)^2} \qquad \{\Delta x = \Delta y\}$$

$$\therefore \ \frac{T^*_{n+1,j} - T_{n+1,j}}{\Delta\tau/2} = \frac{2}{(\Delta x)^2} [T^*_{n,j} - T^*_{n+1,j} \{1 + \frac{ah\Delta x}{k} + \frac{a\lambda k_p B\Delta x}{k}\}$$

$$+ \frac{ah\Delta x}{k} - \frac{a\lambda k_p \Delta x}{k} \{\frac{A - P_a + B\theta_o}{\theta_a - \theta_o}\}]$$

$$+ \frac{T_{n+1,j-1} - 2T_{n+1,j} + T_{n+1,j+1}}{(\Delta x)^2}$$

Let $G1 = \dfrac{ah\Delta x}{k}$

$G2 = \dfrac{a\lambda k_D B\Delta x}{k}$

$R = \dfrac{\Delta\tau}{(\Delta x)^2}$

$\therefore T^*_{n+1,j}\{1+R(1+G1+G2)\} = RT^*_{n,j} + \dfrac{R}{2}[T_{n+1,j-1} + T_{n+1,j+1} - 2T_{n+1,j}$

$$+ 2G1 - \dfrac{2G2}{B}\{\dfrac{A-P_a+B\theta_O}{\theta_a-\theta_O}\}] + T_{n+1,j}$$

Let $E = \dfrac{R}{2}\left[T_{n+1,j+1} + T_{n+1,j-1} - 2T_{n+1,j} + 2G1 - \dfrac{2G2}{B}\{\dfrac{A-P_a+B\theta_O}{\theta_a-\theta_O}\}\right] + T_{n+1,j}$

$\therefore T^*_{n+1,j}\{1 + R(1 + G1 + G2)\} = RT^*_{n,j} + E$

$$T^*_{n+1,j} = \dfrac{RT^*_{n,j}}{1+R(1+G1+G2)} + \dfrac{E}{1 + R(1 + G1 + G2)} \tag{2.13}$$

Equation 2.13 gives the value of $T^*_{n+1,j}$ in terms of $T^*_{n,j}$. Substituting equation 2.13 in the nth equation of the set of tri-diagonal system of equations

$$-T^*_{n-1,j} + bT^*_{n,j} - T^*_{n+1,j} = d_n$$

$$-T^*_{n-1,j} + bT^*_{n,j} - \dfrac{RT^*_{n,j}}{1+R(1+G1+G2)} - \dfrac{E}{1+R(1+G1+G2)} = d_n$$

$$-T^*_{n-1,j} + \{b - \frac{R}{1+R(1+G1+G2)}\}T^*_{n,j} = d_n + \frac{R}{1+R(1+G1+G2)}$$

$$\therefore b_n = b - \frac{R}{1 + R(1 + G1 + G2)}$$

$$d'_n = d_n + \frac{E}{1 + R(1 + G1 + G2)}$$

On modifying the coefficients of the nth equation, the entire set of equations for the jth column can be solved. The procedure may be repeated for successive columns $j = 1$, $j = 2$, ...$j = n$ until all the $T^*_{i,j}$ are found at the end of the first half time step. $T^*_{i,n+1}$ can be directly obtained by the convection boundary condition. The temperature at the end of the second half time step $\Delta\tau$ can be found by applying equation 2.15 for each grid point $j = 1, 2, ...n$ for all i and then for successive rows ($i = 1, 2, ...n$).

The humidity of air in the oven changes as roasting proceeds and this should be taken into consideration in the model. Assuming that a constant pressure (say 1 atmosphere) is maintained inside the oven and since the oven temperature is constant, the total number of moles of air and water vapor in the oven must also remain constant. During the roasting of meat, water is transferred (in the form of vapor) to the air and to prevent the pressure from rising inside the oven, a certain amount of wet air must be vented out of the oven. For the sake of simplicity, it will be assumed that the water vapor evaporated from the meat is thoroughly mixed with the hot air before the mixture is vented.

If the oven is completely dry at the start of roasting

$\therefore \quad P_a = 0$ at t = 0

Let ρ_a be the density of gas (kg/m^3) at temperature θ_a and V be the volume of the oven (m^3).

$\therefore$ Mass of dry air at t = 0 = $M_a = \rho_a V$ kg

Total moles of dry air = $M_t = \dfrac{\rho_a V}{29.0}$ kg-moles

Let ΔW be the mass of water (kg) which is evaporated from the meat in the time interval Δt.

$$\Delta W = k_p (P_S - P_a) a' \cdot \Delta t \qquad\qquad (2.14)$$

where $P_S = A + B\theta$

   a' = total surface area of meat (m^2)

$\therefore$ Mass of water vapor in the oven = $W = W' + \Delta W$ (W' = 0 at t = 0)

Moles of water vapor in the oven = $M_w = W/18.0$

Mass of air in the oven = M_a

Moles of air in the oven = $M_a/29.0$

Total Moles of air and water vapor = M_t

Moles of air and water vented = $M_v = M_a/29.0 + W/18.0 - M_t$

Mass of water vapor removed = $\dfrac{W}{M_t} * M_v$

Mass of air removed = $\dfrac{M_a}{M_t} * M_v$

Hence Mass of water vapor remaining inside the oven

$$= W' = W \left\{1 - \frac{M_v}{M_t}\right\}$$

Mass of air ramaining in the oven $M'_a = M_a \left\{1 - \dfrac{M_v}{M_t}\right\}$

Humidity in the oven = $H = \dfrac{W'}{M'_a}$

We know that $H = \dfrac{18.0 * P_a}{29.0 * (P - P_a)}$

$$\therefore \quad P_a = \frac{H * 29.0 * P}{18.0 + H * 29.0} \qquad (2.15)$$

Where P is the total pressure = 1.03×10^5 Pascals. The value of P_a at the end of time interval Δt is given by equation 2.15 and this value of P_a can be used in equation 2.14 to calculate the amount of water evaporated in the next time step.

Begin → Read input variables and set values for $\Delta\tau$, Δx and # of grid pts → Initialize the Temp. of all the grid pts, set $P_a = 0$ and $W' = 0$

Repeat for all values of $j=1,2,...m$

Compute d_i

$d_i = T_{i,j-1}$ +

$2 \{\frac{(\Delta x)^2}{\Delta\tau} -1\} T_{i,j}$

$+ T_{i,j+1}$

$i = 1,2,...n$

$C_1 = -2$

$\tau = \gamma + \Delta\tau$

*

Set coefficient of the tridiagonal matrix

$a_i = -1$

$b_i = 2(\frac{(\Delta x)^2}{\Delta\tau} + 1)$

$c_i = -1$

Modify value of d_n and b_n → Solve the tridiagonal set of equations with coeff. a_i, b_i, c_i, d_i $i=1, 2, ..n$

Solve the tridiagonal set of equations with coeff. e_j, b_j, c_j, d_j $j=1,2...m$ ← Modify value of d_m and b_m ← Compute d_i for next time step $d_j = T^*_{i-1,j} +2\{\frac{(\Delta x)^2}{\Delta\tau} -1\} T^*_{i,j}$ $+ T^*_{i+1,j}$ $j = 1,2,...m$

Repeat for all values of $i=1,2,...n$

Compute Δw $= k_p a' \Delta\tau (P_s - P_a)$ → Find Hum and P_a at the end of time interval $\Delta\tau$. → Check if Center Temp $\le T_{max}$ — F → Stop

GOTO*
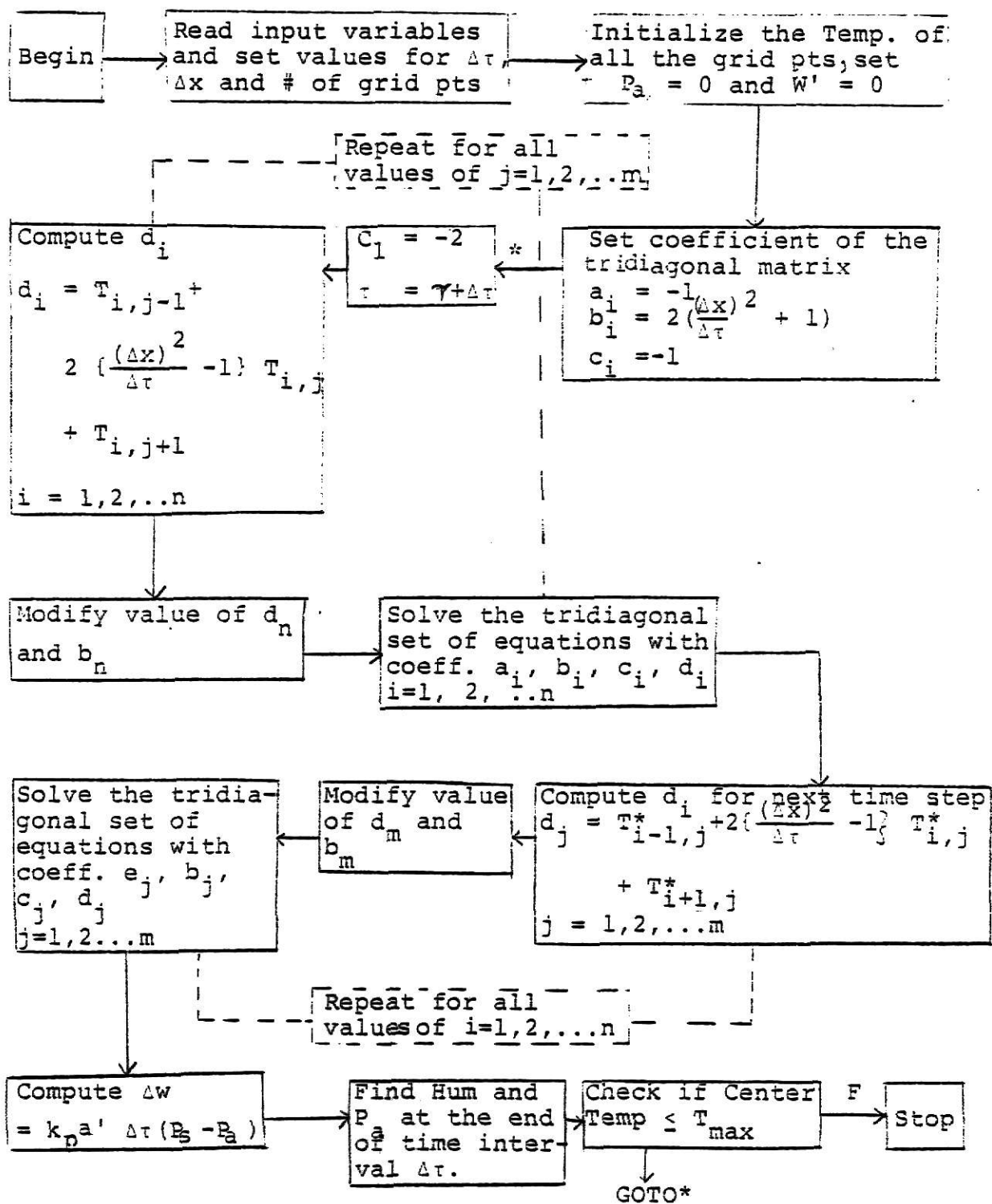
Fig. 2.3. Flow diagram of the simulation for the roasting of meat.

III. RESULTS AND DISCUSSION

Computer simulations were carried out for two different oven temperatures, $175^\circ C$ and $225^\circ C$. The computer program is given in the appendix. Table 3.1 summarizes the results as the length of time for the center to reach $40^\circ C$ and $70^\circ C$. The cooking parameters used in the simulations were obtained from the literature. The thermal conductivity of beef was taken to be 0.4 watts/m^2 $^\circ C$ [8,9] and the density and specific heat as 879 kg/m^3 and 2510 J/kg$^\circ C$, respectively [9,10]. Based on the above values, the thermal diffusivity $(k/_\rho c_p)$ was found to be 1.8×10^{-7} m^2/sec. The results from the computer simulations were compared with the experimental results given by Bengtsson et al. [6]. For the purpose of comparison, the dimension of the meat and the heat transfer coefficient h were taken to be the same as that chosen by the above authors [6]. The mass transfer coefficient k_p was obtained by the relationship between the heat and mass transfer during drying ($h/k_p \lambda$ = 64.7) [7].

Table 3.1. Comparison of calculated and experimental cooking time for oven temperatures 175°C and 225°C

Oven Temp. (°C)	Initial Temp. (°C)	Final Center Temp. (°C)	Experimental Cooking time (min)	Calculated Cooking time (min)
175.0	5.0	40.0	39.0	41.0
		70.0	80.0	70.0
225.0	5.0	40.0	32.0	32.5
		70.0	60.0	50.0

Figures 3.1, 3.2 and 3.3 show a relationship between the wet bulb temperature T_w, the surface temperature T_s and the center temperature T_c. The nature of these curves are very similar to those shown by Bengtsson et al. [6]. The center temperature, the wet bulb temperature and the surface temperature increased monotonically with the cooking time. The wet bulb temperature increases due to the accumulation of steam in the oven. The surface temperature moved closer to the wet bulb temperature towards the end of the cooking period. The falling rate period of drying starts when the surface temperature exceeds the wet bulb temperature. For an oven temperature of $175^{\circ}C$ and a heat transfer coefficient of 5 watts/m^2 $^{\circ}C$, the surface temperature always remained less than the wet bulb temperature. For this case the constant drying rate prevailed during the entire cooking. Increasing the heat transfer coefficient from 5 to 30 watts/m^2 $^{\circ}C$ simultes forced convection cooking. This is shown in Figure 3.3. Since the heat transfer coefficient was increased significantly, the rate of heating increased and consequently the surface temperature rose very sharply. The surface temperature became greater than the wet bulb temperature and the constant drying rate period was reduced to about 7 min. of cooking time. It was followed by the first falling rate period. At the end of the constant drying period and the start of the falling rate period (Fig. 3.3), the surface temperature exceeds T_w and also $100^{\circ}C$, indicating a formation of crust at the meat surface. Keeping the heat transfer coefficient the same as in case 1 (5 watts/m^2 $^{\circ}C$) and

increasing the oven temperature to 225°C, reduced the constant

drying period to 30 minutes (Fig. 3.2). Again as in Figure

3.3 (h = 30 watts/m^2 °C and T_a = 175°C) the surface temperature

exceeds 100°C.

Figure 3.4 compares the moisture loss as a function of

cooking time for the oven temperatures of 175°C and 225°C.

The moisture loss curve for an oven temperature of 175°C is

almost linear, therefore, the constant drying rate period pre-

vailed during the entire cooking. For an oven temperature of

225°C, there was an abrupt change in the shape of the curve

after 30 minutes of cooking, indicating the start of the

falling rate period. The moisture loss when the meat was

medium cooked (T_c = 70°C) was about doubled when the oven temp-

erature was 225°C. Increasing the oven temperature from 175°C

to 225°C caused a 15% reduction in the cooking time (Fig. 3.5)

but also doubled the moisture loss.

Moisture loss is an important factor in the cooking of

meat and it should be taken into account in the numerical

model describing the roasting process. For an oven tempera-

ture of 225°C and a heat transfer coefficient of 5 watts/m^2 °C,

21.8 gm of moisture per 600 gm of meat was evaporated from

the meat surface for the center temperature to reach 70°C.

The energy required for evaporating this water was 53 kJ and

it was approximately 30% of the total energy required for

cooking. (For T_a = 175°C and h = 5 watts/m^2 °C, approximately

25% of the total energy required for cooking was used for

evaporating the moisture). Melting of fat is not very

critical as far as the energy requirement for the roasting is concerned. The fat content in meat varies from 1.3% to 10% and only a part of this fat melts and drips to the bottom. The meat sample used by Bengtsson et al. [6] had a fat content of 4% or lower. The amount of energy required to melt all the fat would only be about 3% of the total energy required for the meat to be medium cooked (T_c = 70°C). As a result, the melting of fat does not appreciably change the energy requirement in this model.

Figures 3.5 and 3.6 show how the center temperature changed with time for various values of the heat transfer coefficient and oven temperature. The general shape of the curve was not altered by changing the cooking variables (h and T_a). These curves were almost flat at the beginning of cooking but they rose very rapidly about half-way through the cooking period. They again tended to flatten out towards the end of cooking. As seen from Figure 3.6, increasing the heat transfer coefficient from 5 watts/m^2 °C to 10 watts/m^2 °C decreased the cooking time by almost 35% (T_c = 70°C). Further increasing the heat transfer coefficient to 30 watts/m^2 °C casued a further decrease of cooking time by another 15.0% for the meat to be cooked medium. Similar results were obtained when the oven temperature was increased to 225°C.

Table 3.1 compares the experimental and simulated cooking time for the center temperature to reach 40°C and 70°C for two different oven temperatures. Figure 3.7 compares the experimental and simulated center temperature of the meat as a

function of cooking time for an oven temperature of $175^{O}C$. As seen from Table 3.1 and Figure 3.7, there was close agreement between the experimental and simulated results until the center temperature reached $40^{O}C$. The difference between the two showed up when T_c became greater than $40^{O}C$. The difference was primarily caused by the evaporation of water from the meat surface as cooking progressed. Due to this transport of moisture, the water content decreased and, as a result, the thermal conductivity of the meat decreased. This changed the thermal diffusivity which in turn caused the experimental cooking time to be greater than the simulated cooking time. Another reason for this slight difference was the formation of crust. As seen from Figures 3.1 and 3.2, the surface temperature approached $100^{O}C$ towards the end of cooking and this marked the formation of crust. Since the water content in the crust is much lower than the rest of the meat [4], the thermal conductivity of the crust is significantly lower. This increased the resistance to the flow of heat to the meat.

When the meat was cooked at an oven temperature of $225^{O}C$, the surface temperature T_s exceeded the wet bulb temperature T_w after about 35 minutes of cooking (Figure 3.2). As a result, a transition from the constant drying rate period to the falling rate period took place. Due to this transition, the heat transfer coefficient decreased markedly which caused the experimental cooking time to increase.

Several researchers have found that proteins denature when the meat is heated to a temperature of about $50-60^{O}C$.

Protein denaturation results in a sudden release of water from the muscle. It is not very clear what effect this release of meat juices has on the roasting of meat. Godsalve et al. [2] pointed out that sometimes protein denaturation causes a decrease in the temperature near the surface (region where the juice is being released). Denaturation of proteins also alters the porous structure [2] which in effect changes the basic mechanism of moisture migration. The effect of this phenomenon on the thermal conductivity of meat is not very well understood.

Figures 3.8 to 3.11 give the 40^OC and 70^OC isotherms inside the meat piece at different levels of cooking time. Due to the symmetry of the problem, the isotherms are shown only for one quadrant. Point A in Figure 3.8 refers to the center of the meat. Sides BC and DC were exposed to the convective boundary condition. Figure 3.8 shows the 40^OC isotherms within the meat, when the oven was operated at 175^OC and the heat transfer was by free convection (h = 5 watts/m^2 ^{O}C). Figure 3.8 shows how the 40^OC temperature isotherm moved towards the center of the meat piece as cooking progressed. Figure 3.9 shows the same isotherm but for a higher oven temperature of 225^OC. As seen from Figures 3.8 and 3.9, the 40^OC isotherm penetrated much faster for the higher oven temperature. It took only about 32 min. for an oven temperature of 225^OC as compared to 41 min. for an oven temperature of 175^OC for the center temperature to reach 40^OC. This resulted in a

decrease of approximately 25% in the cooking time. Thus, cooking time can be reduced significantly by raising the oven temperature, but at the expense of greater moisture loss as shown in Figs. 3.4 and 3.5. Figures 3.10 and 3.11 show the $70^{\circ}C$ isotherms for T_a = $175^{\circ}C$ and $225^{\circ}C$ and similar conclusions were reached.

Figures 3.12 to 3.18 show different temperature levels (20-80$^{\circ}C$) that existed in the meat at fixed times (h = 5 w/m^2 $^{\circ}C$ and T_a = $175^{\circ}C$). After 10 min. of cooking (Fig. 3.12), the maximum temperature in the meat was $40^{\circ}C$ (which is the temperature at the outer corner). After 20 minutes, the $20^{\circ}C$ isotherm had moved closer to the center and had penetrated faster than the $30^{\circ}C$ isotherm.

Proteins denature when they are heated to about 60-70$^{\circ}C$. Protein denaturation results in a sudden release of moisture and it is of considerable importance in understanding the mechanism of moisture migration inside the meat. From these isotherms it is possible to tell which region inside the meat will be releasing moisture due to protein denaturation. This region will have an increased moisture content and therefore an increased thermal conductivity relative to the condition prior to denaturation. The meat was $60^{\circ}C$ after approximately 30 min of cooking (Fig. 3.14). The portion of the meat below the $60^{\circ}C$ isotherm is at a temperature higher than $60^{\circ}C$. The region between $60^{\circ}C$ isotherm and $50^{\circ}C$ isotherm (Fig. 3.15) is the region where release of juices is taking place. This zone moves closer to the center as cooking progresses. A

similar set of figures, for the oven temperature of 225°C (and h - 5 watts/m^2 ^{O}C), are given in the appendix. For an oven temperature of 225°C, the actual cooking times may be somewhat longer than the simulated cooking times for the same center temperature because the effect of moisture loss on thermal conductivity is not included in the mathematical model.

Fig. 3.1 Simulation results showing the relationship between the Wet Bulb Temperature (T_w), Surface Temperature (T_s) and Center Temperature (T_c) for h = 5.0 watts/m^2 $^{\circ}$C and T_a = 175°C.
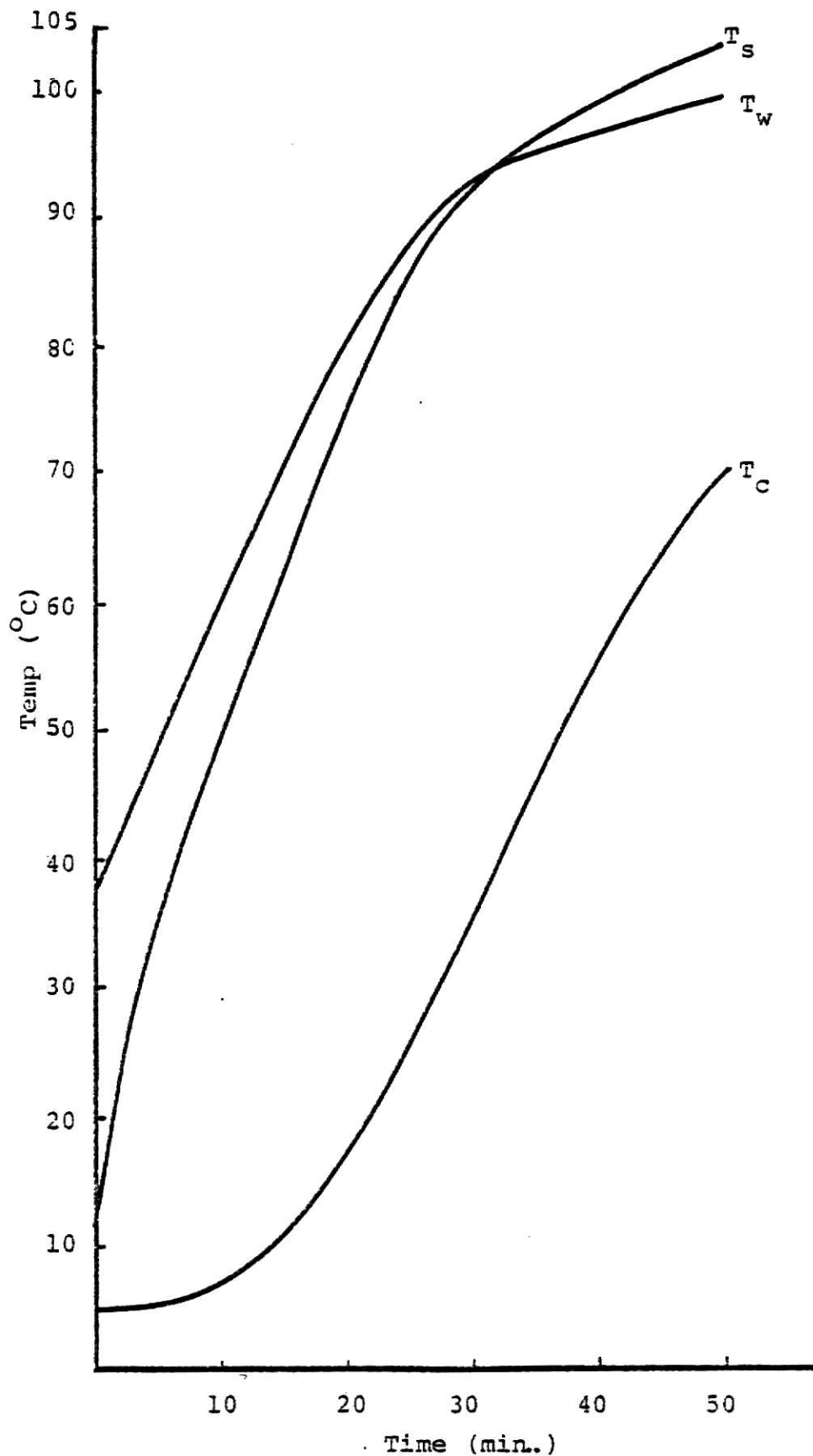
Fig. 3.2. Simulation results showing the relation-
ship between the Wet Bulb Temperature (T_w),
Surface Temperature (T_s) and Center Tem-
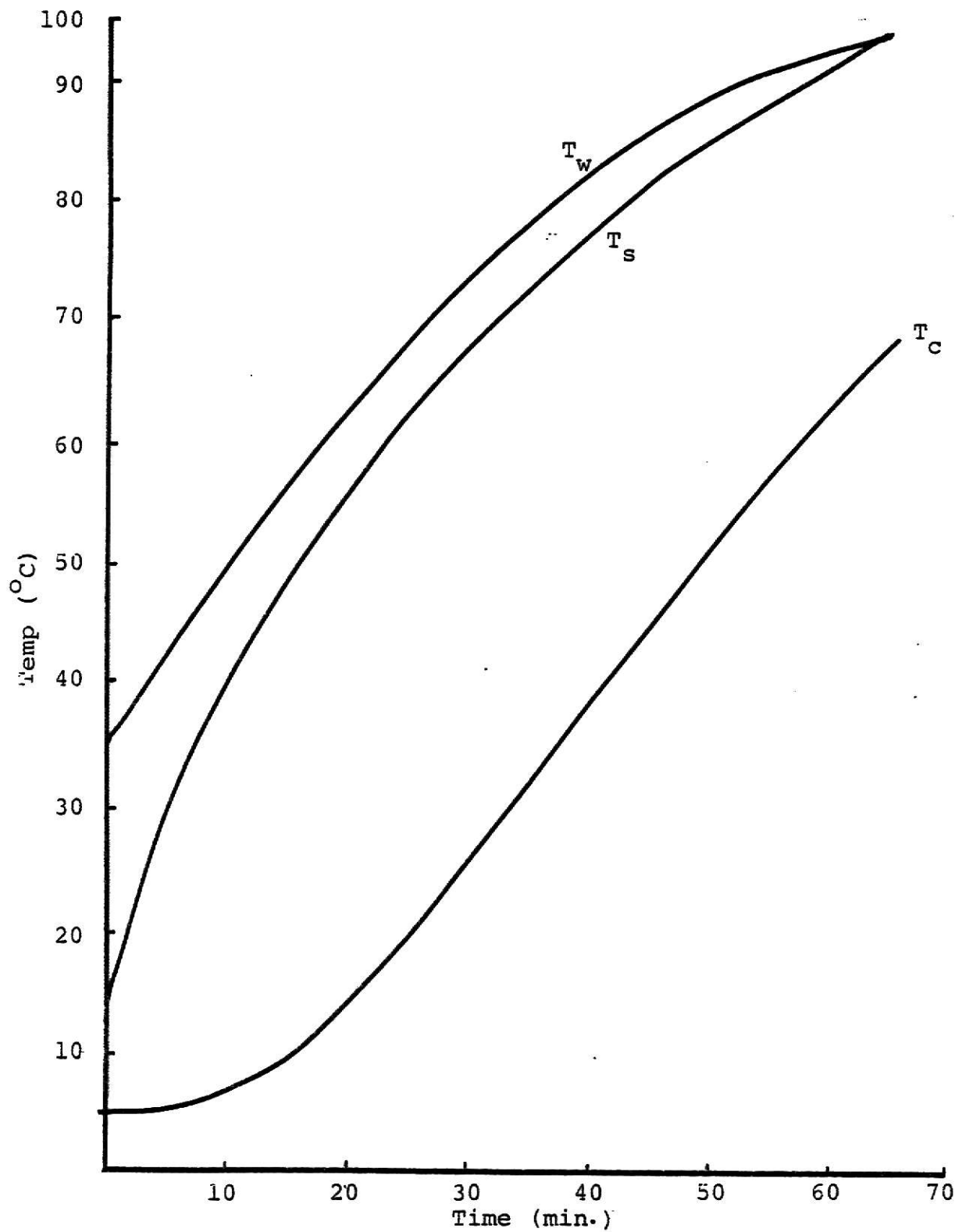perature (T_c) for h=5.0 watts/m^2 $^\circ$C and
T_a = 225°C
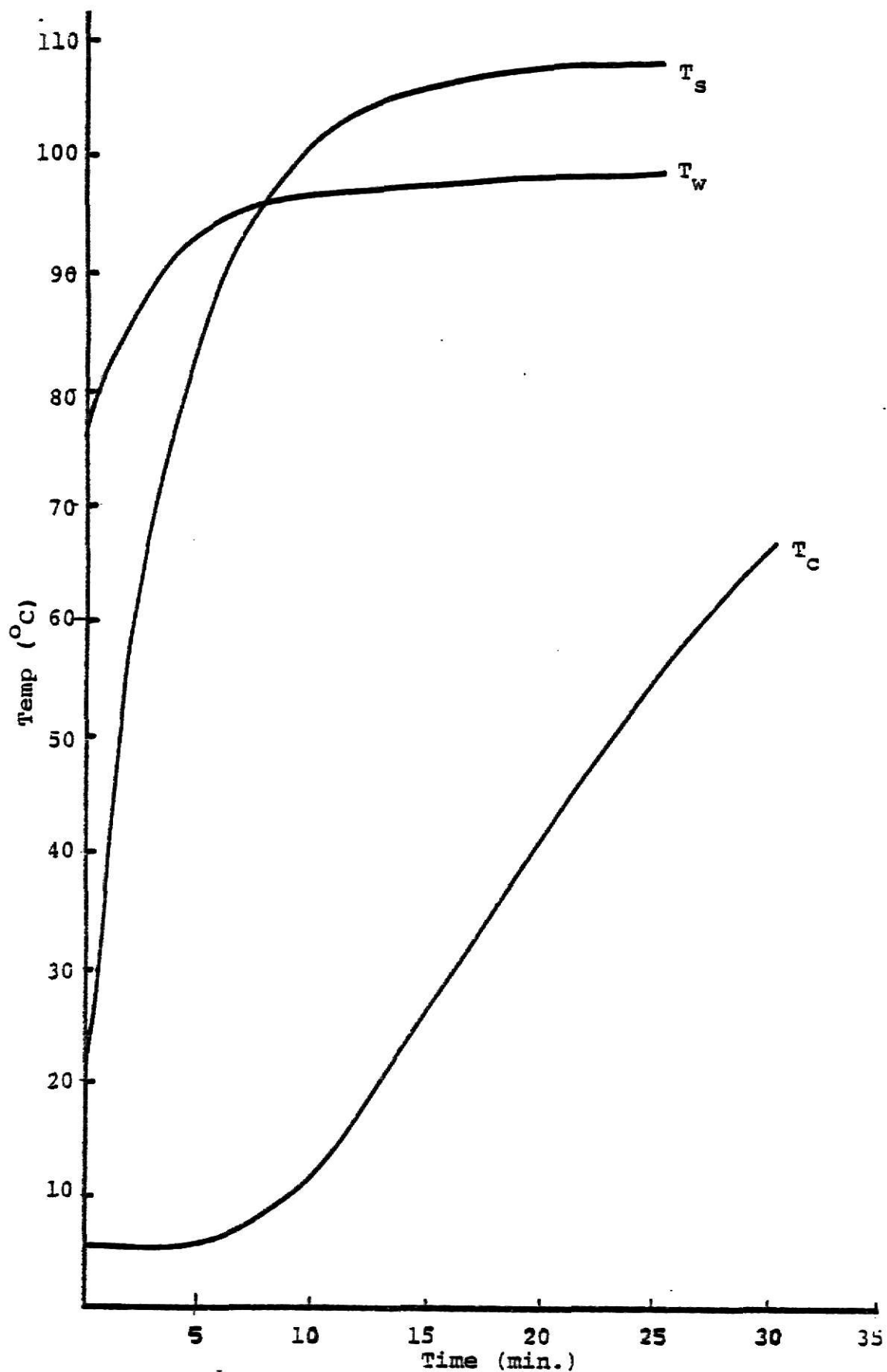
Fig. 3.3. Simulation results showing the relationship
between the Wet Bulb Temperature (T_w), Sur-
face Temperature (T_s) and Center Temperature
(T_c) for h = 30 watts/m^2 ^oC and T_a = 175^oC.
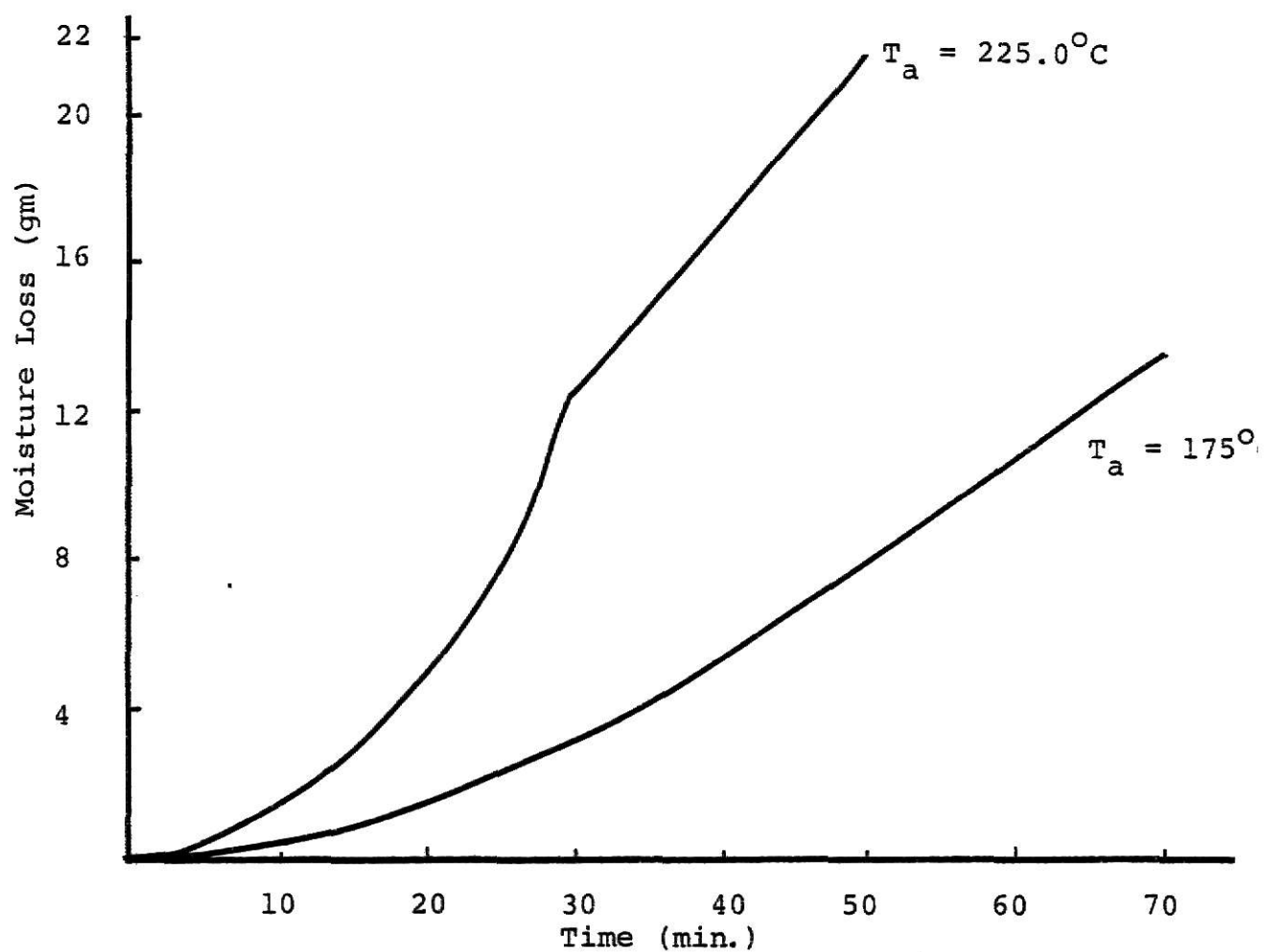
Fig. 3.4.   Simulation results showing the moisture loss as a function of time for $T_a = 175°C$, $T_a = 225°C$ and $h = 5.0$ watts/m^2 $°C$.
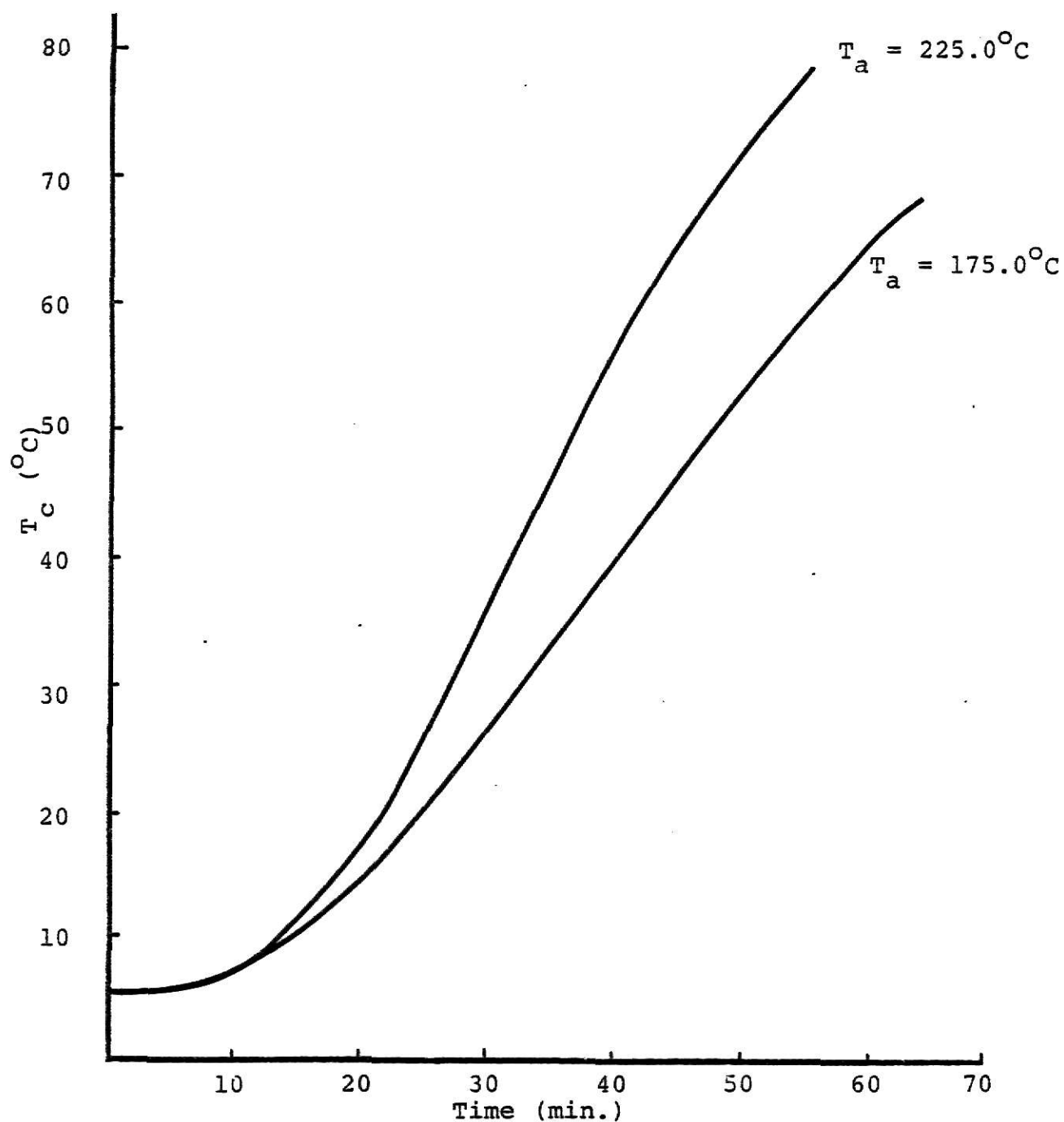
Fig. 3.5. Simulation results showing the Center Temperature as a function of time for two different oven temperatures ($T_a = 175^{\circ}$C, $T_a = 225^{\circ}$C, and $h = 5.0$ watts/m^2 $^{\circ}$C).
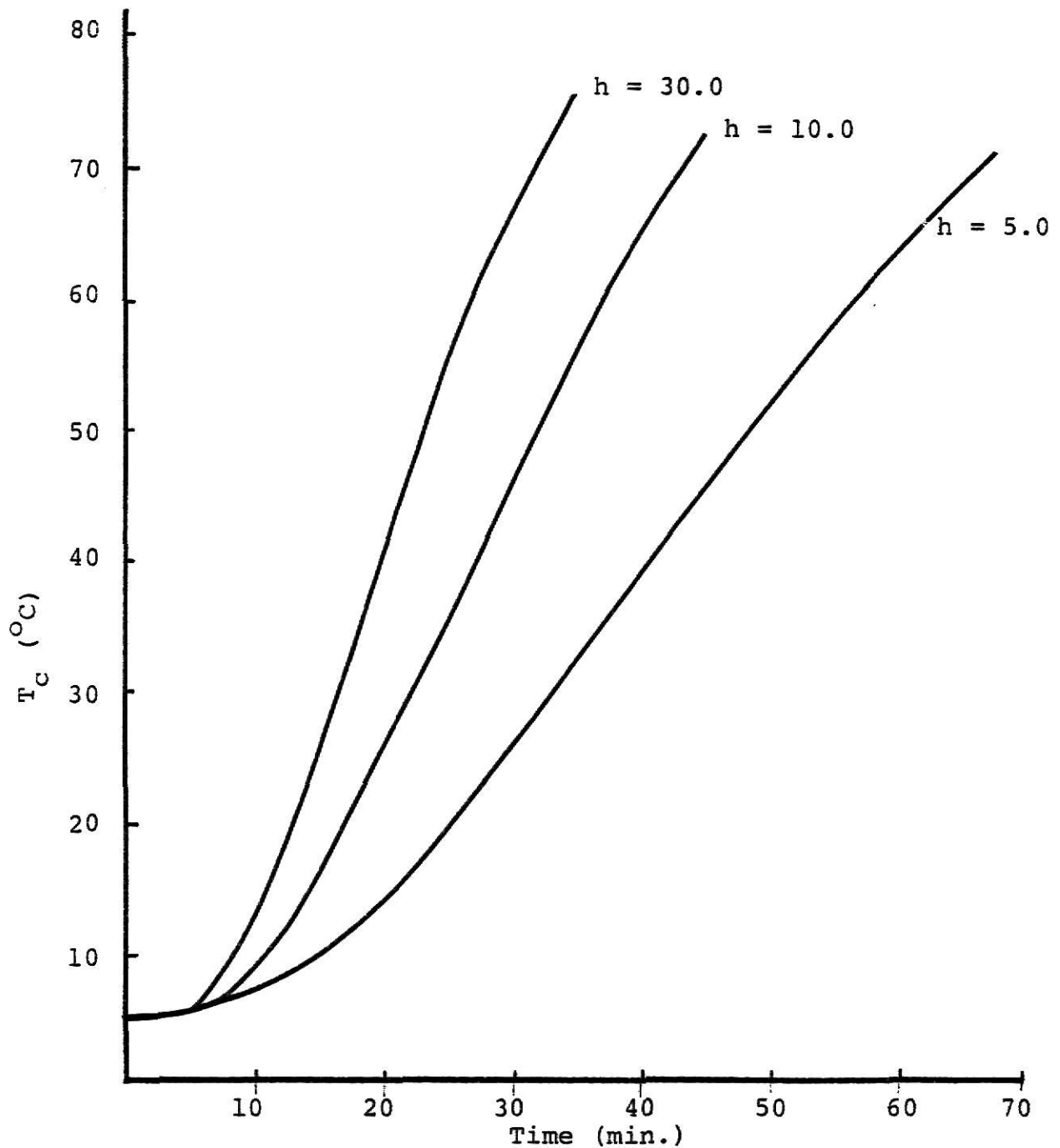
Fig. 3.6. Simulation results showing the Center Temperature as a function of time for different values of Heat Transfer Coefficient (h = 5.0 watts/m^2 ^{o}C, 10.0 watts/m^2 ^{o}C, and 30.0 watts/m^2 ^{o}C) and T_a = 175°C.
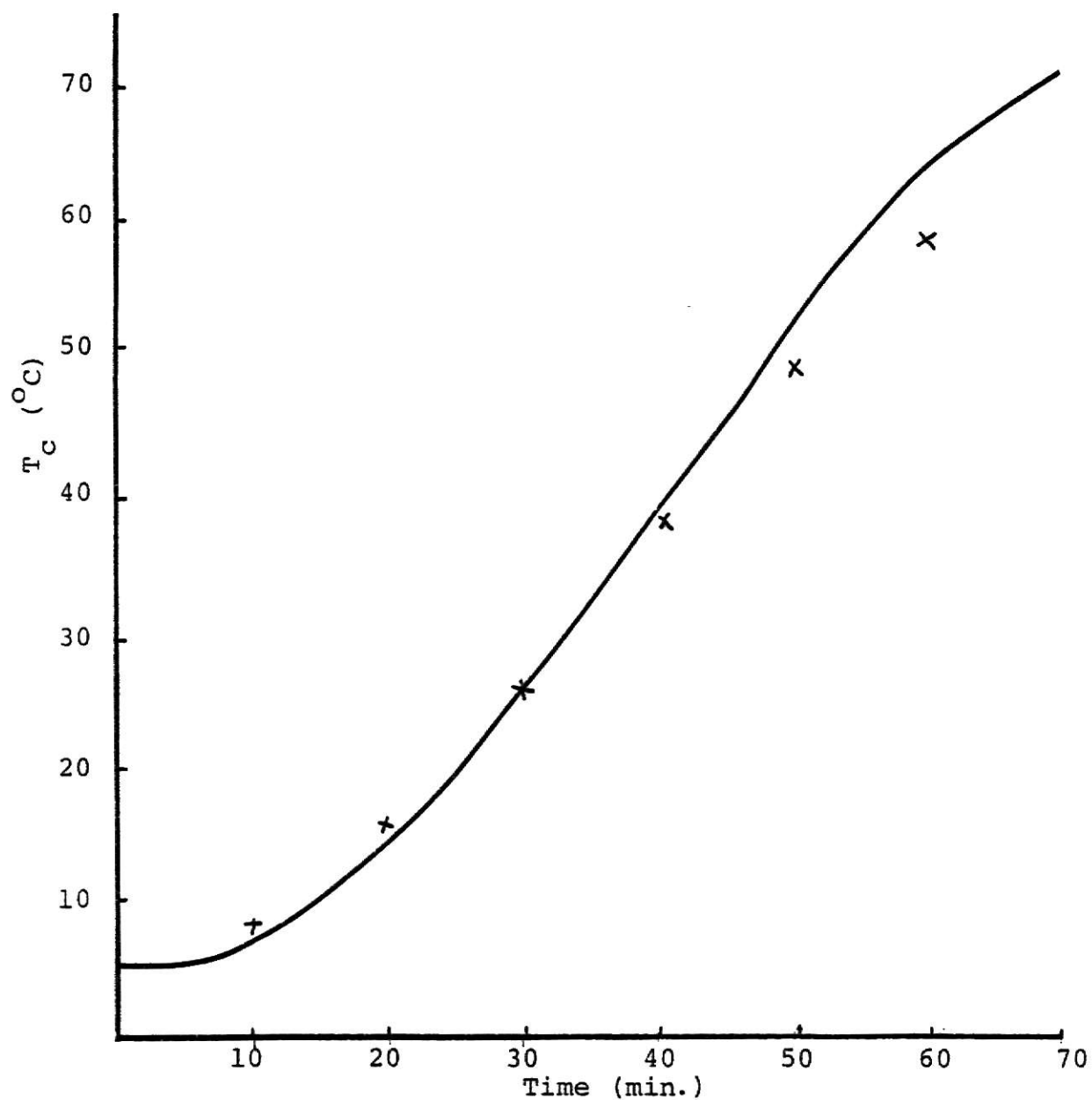
Fig. 3.7. Comparison of simulated Center Temperature
(solid line) and Experimental Center Tempera-
ture (crosses) as a function of time for
$h = 5.0$ watts/m^2 $^{\circ}C$ and $T_a = 175^{\circ}C$.
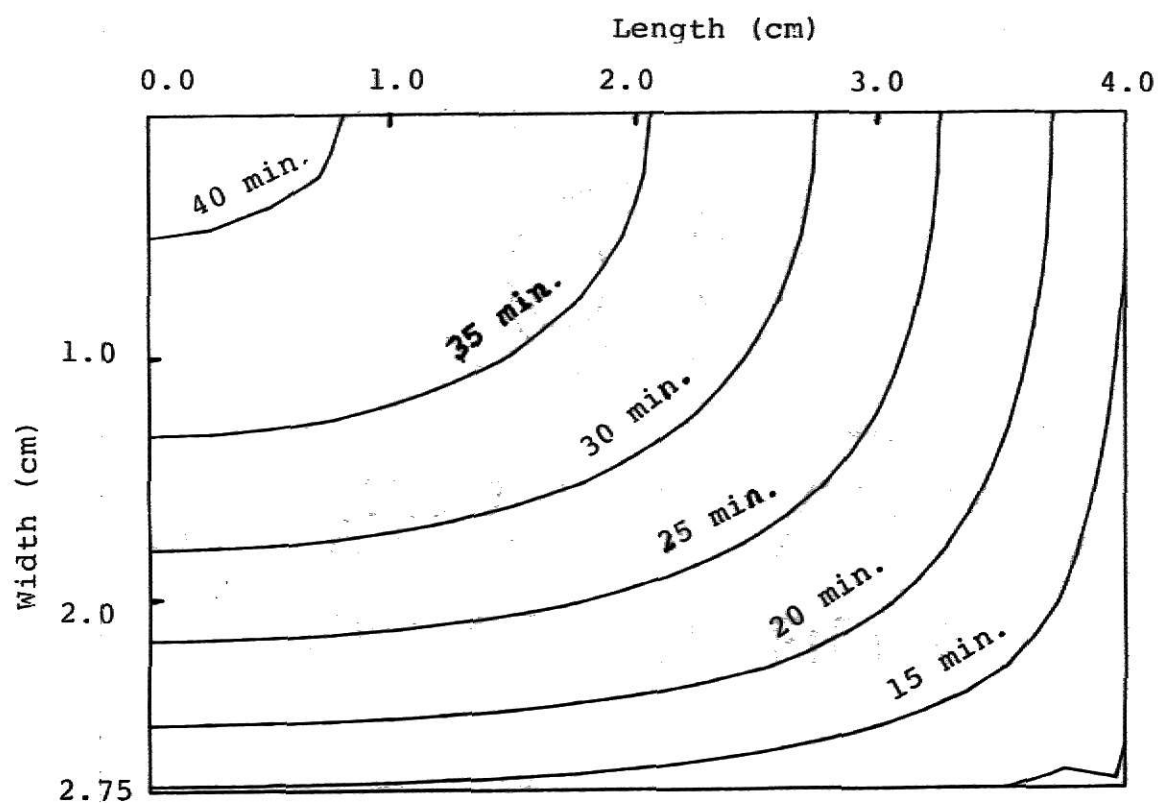
Fig. 3.8. Simulated 40°C temperature profiles at various levels of cooking time for an oven temperature of 175°C. The origin represents the center of the meat piece.
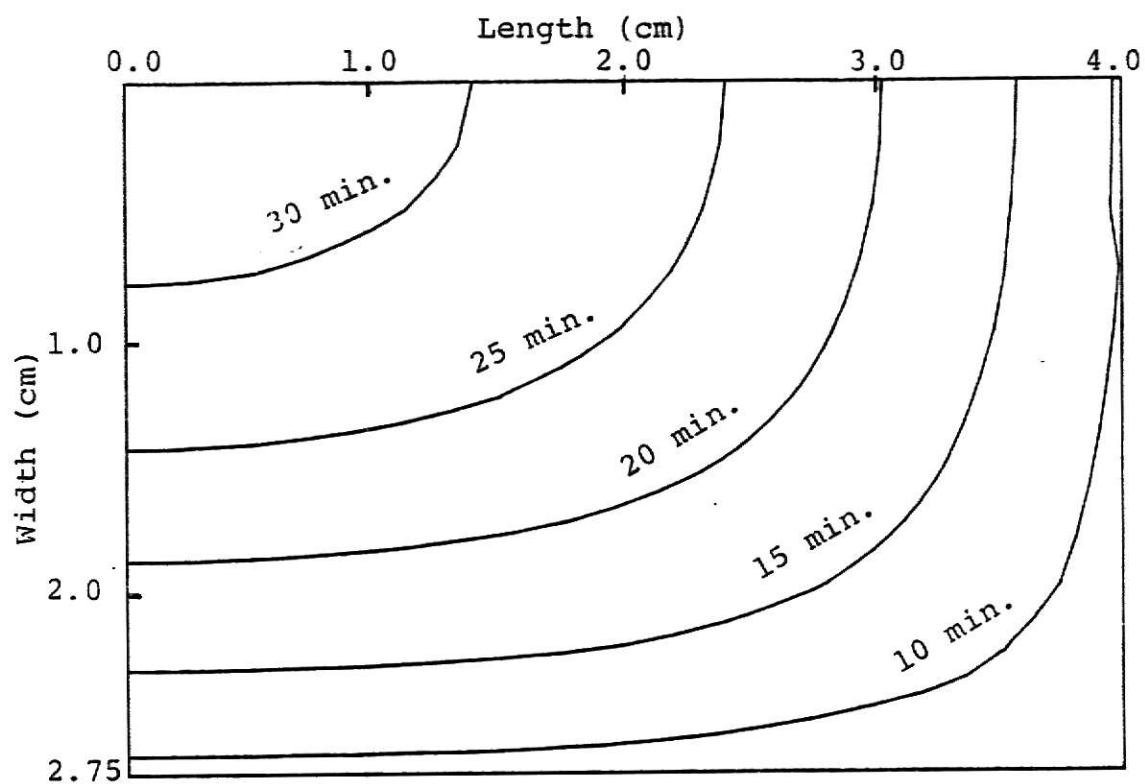
Fig. 3.9. Simulated 40°C temperature profiles at various levels of cooking time for an oven temperature of 225°C. The origin represents the center of the meat piece.
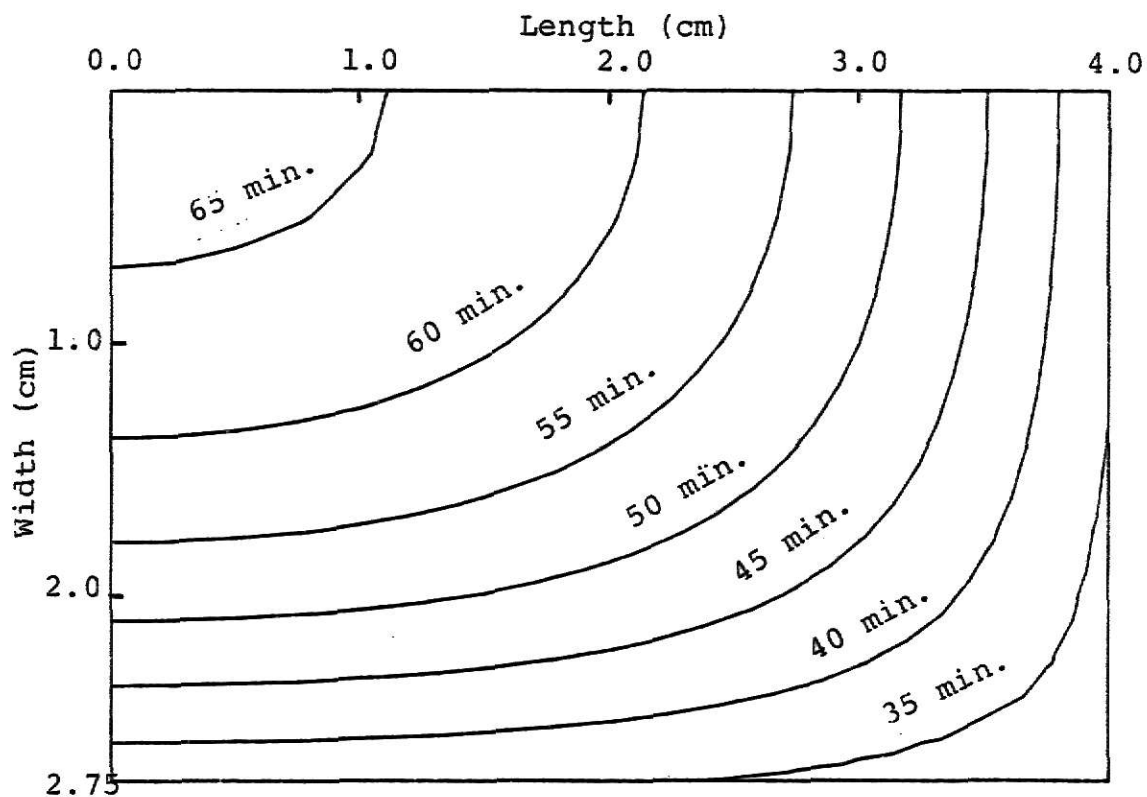
Fig. 3.10. Simulated 70°C temperature profiles at various levels of cooking time for an oven temperature of 175°C. The origin represents the center of the meat piece.
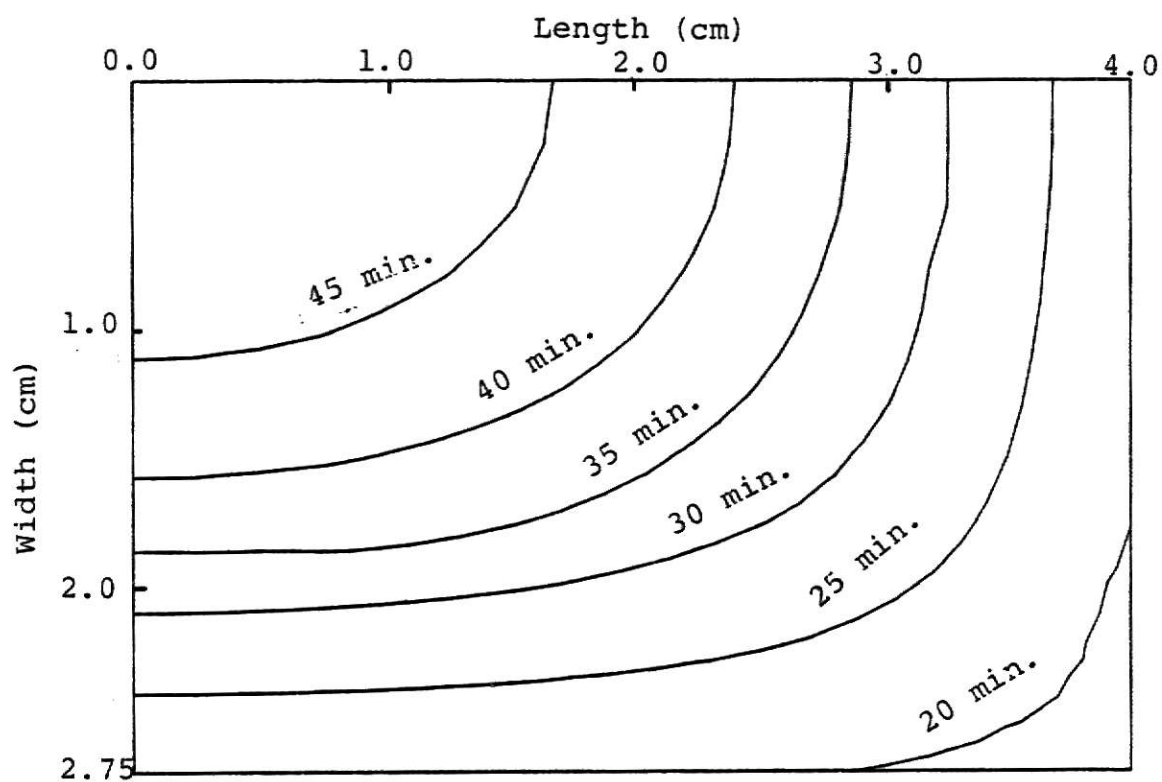
Fig. 3.11. Simulated 70°C temperature profiles at
various levels of cooking time for an
oven temperature of 225°C. The origin
represents the center of the meat piece.

Length (cm)

0.0   1.0   2.0   3.0   4.0
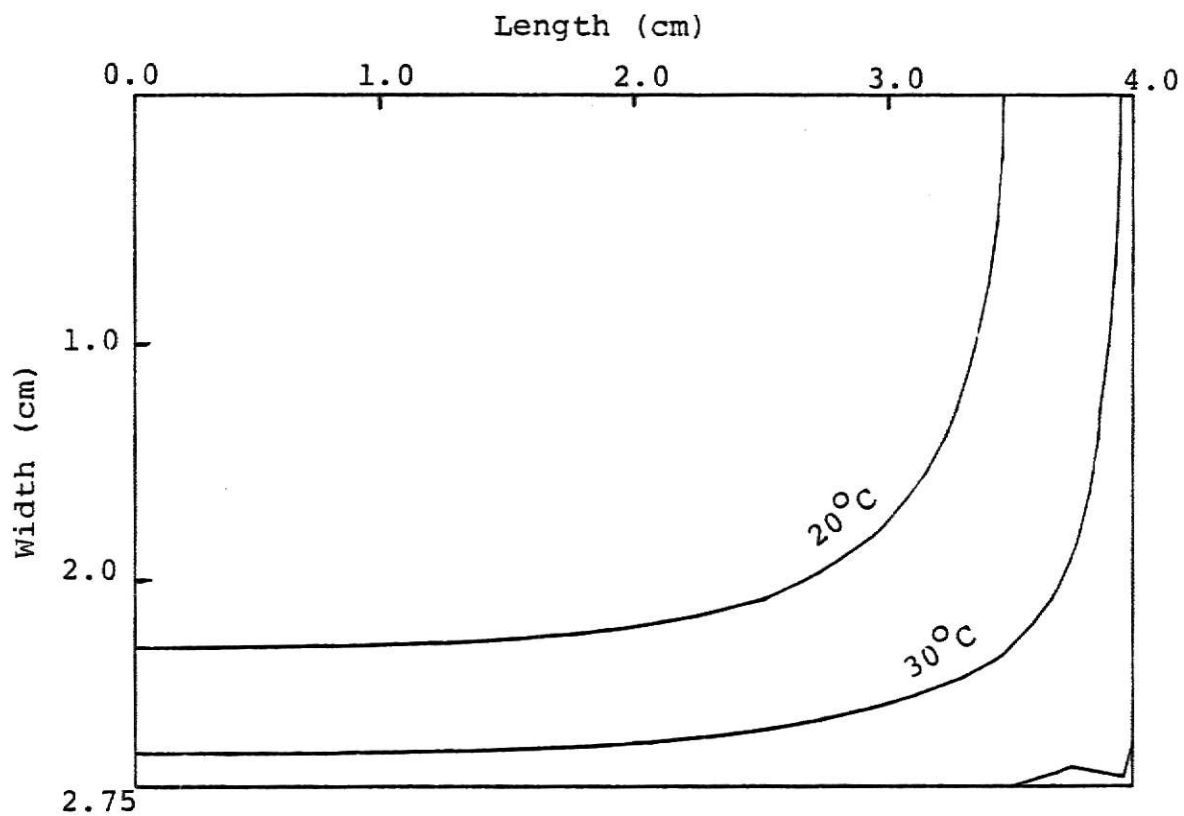
Fig. 3.12.   Simulated temperature profiles for an
             oven temperature of 175°C after 10 min.
             of cooking.   The origin represents the
             center of the meat piece.
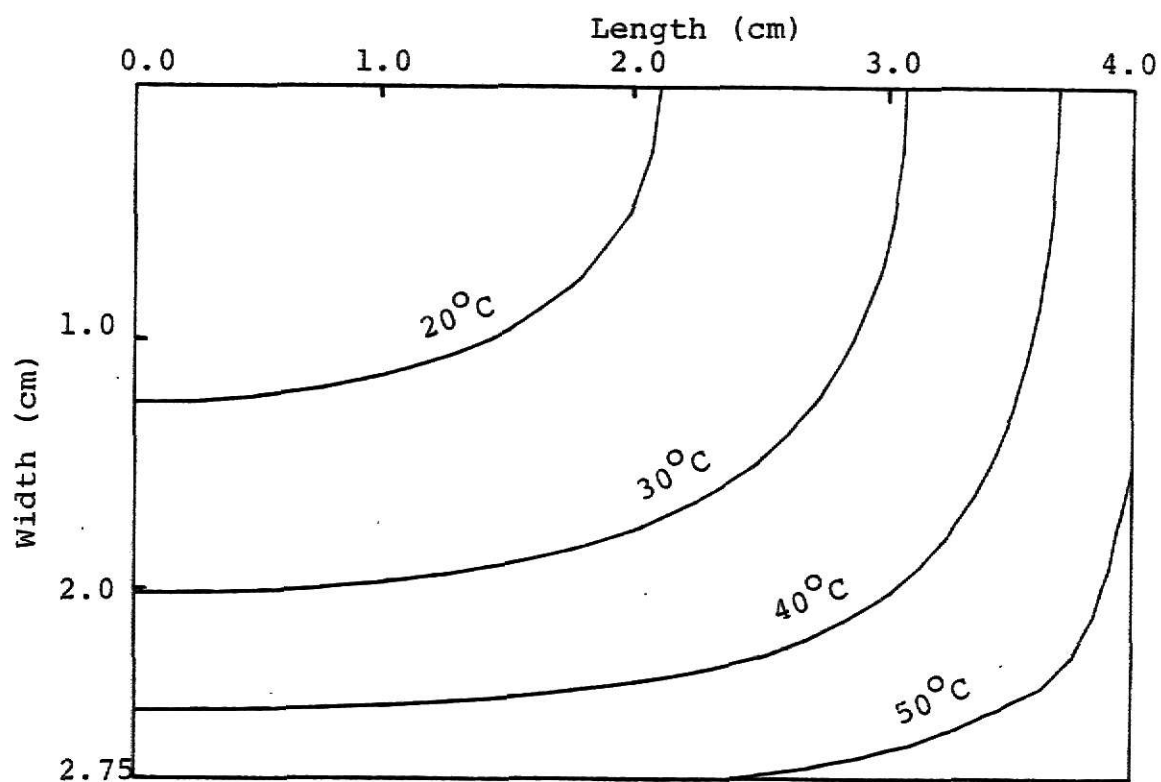
Fig. 3.13. Simulated temperature profiles for an
oven temperature of 175°C after 20 min.
of cooking. The origin represents the
center of the meat piece.
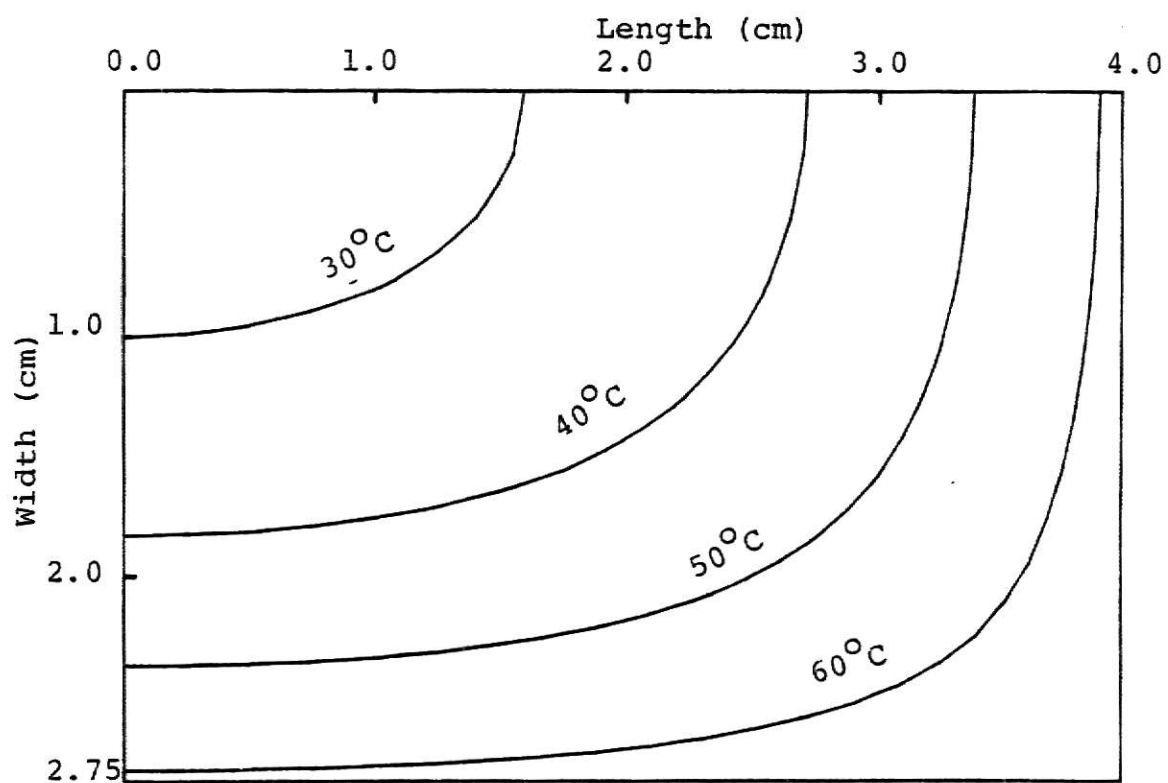
Fig. 3.14. Simulated temperature profiles for an oven temperature of 175°C after 30 min. of cooking. The origin represents the center of the meat piece.
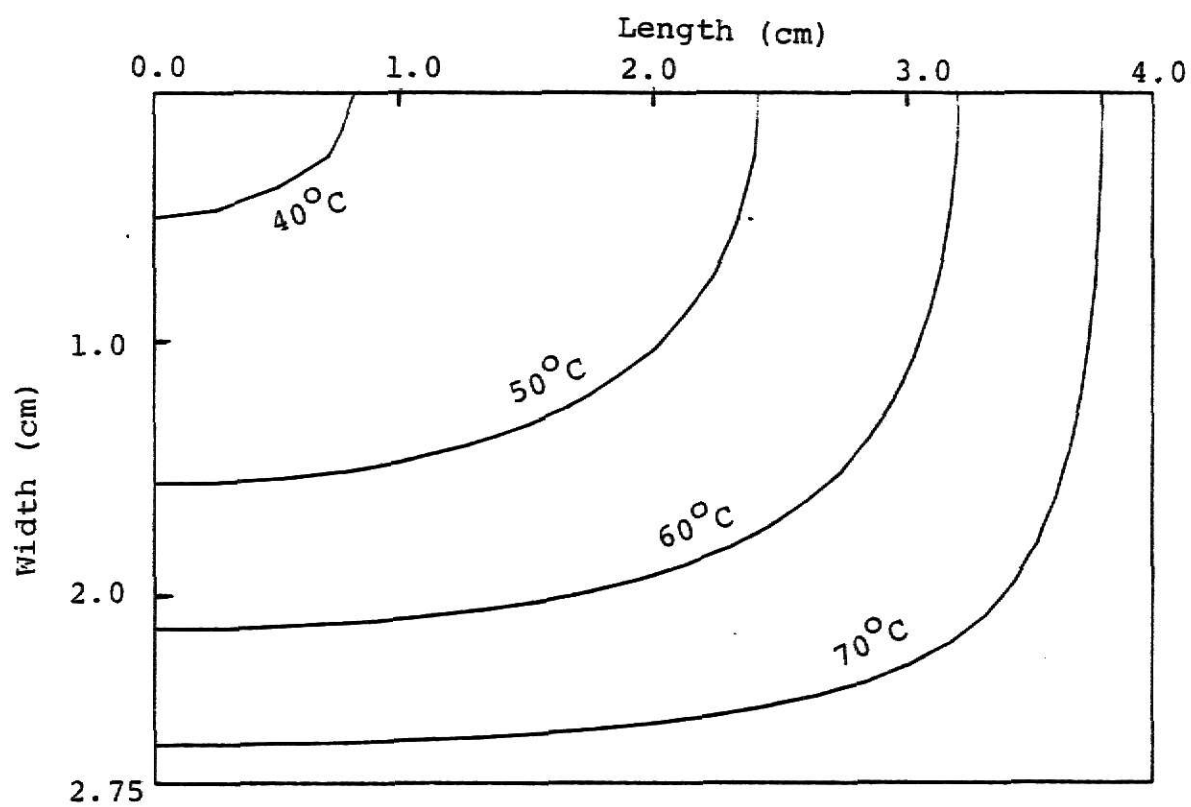
Fig. 3.15. Simulated temperature profiles for an oven temperature of 175°C after 40 min. of cooking. The origin represents the center of the meat piece.
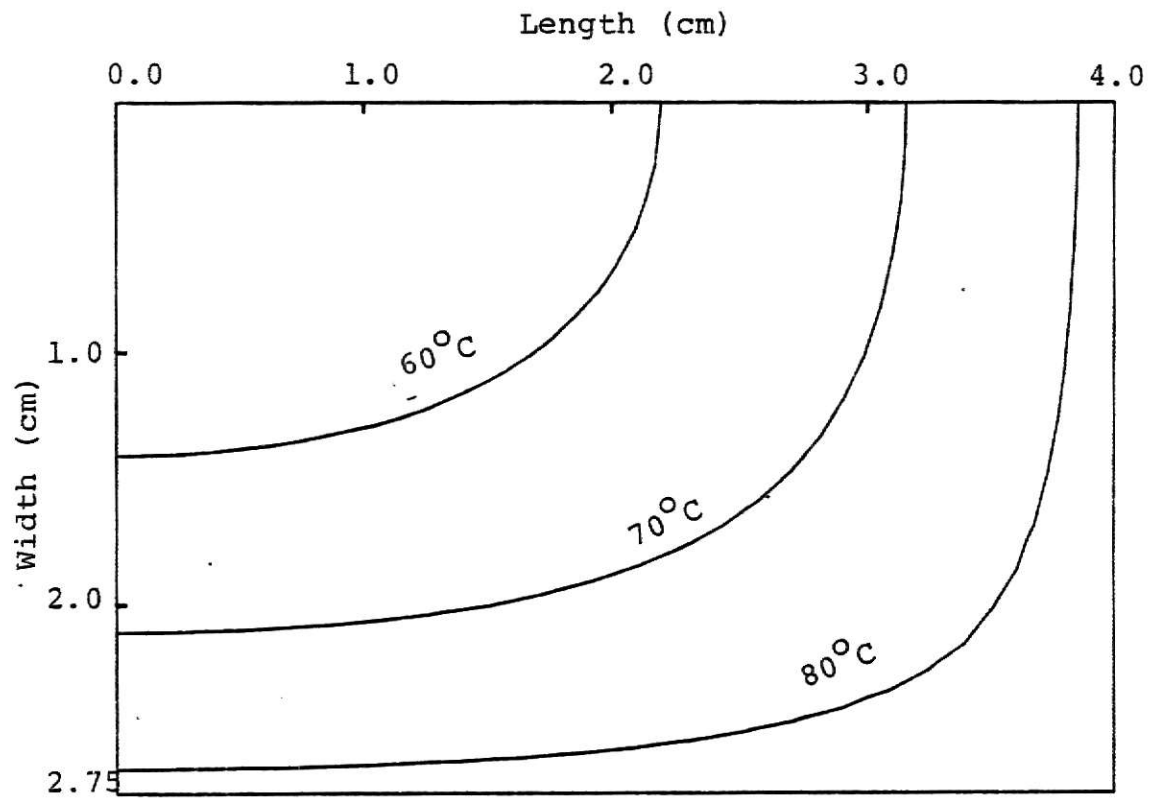
Fig. 3.16. Simulated temperature profiles for an oven temperature of 175°C after 50 min. of cooking. The origin represents the center of the meat piece.
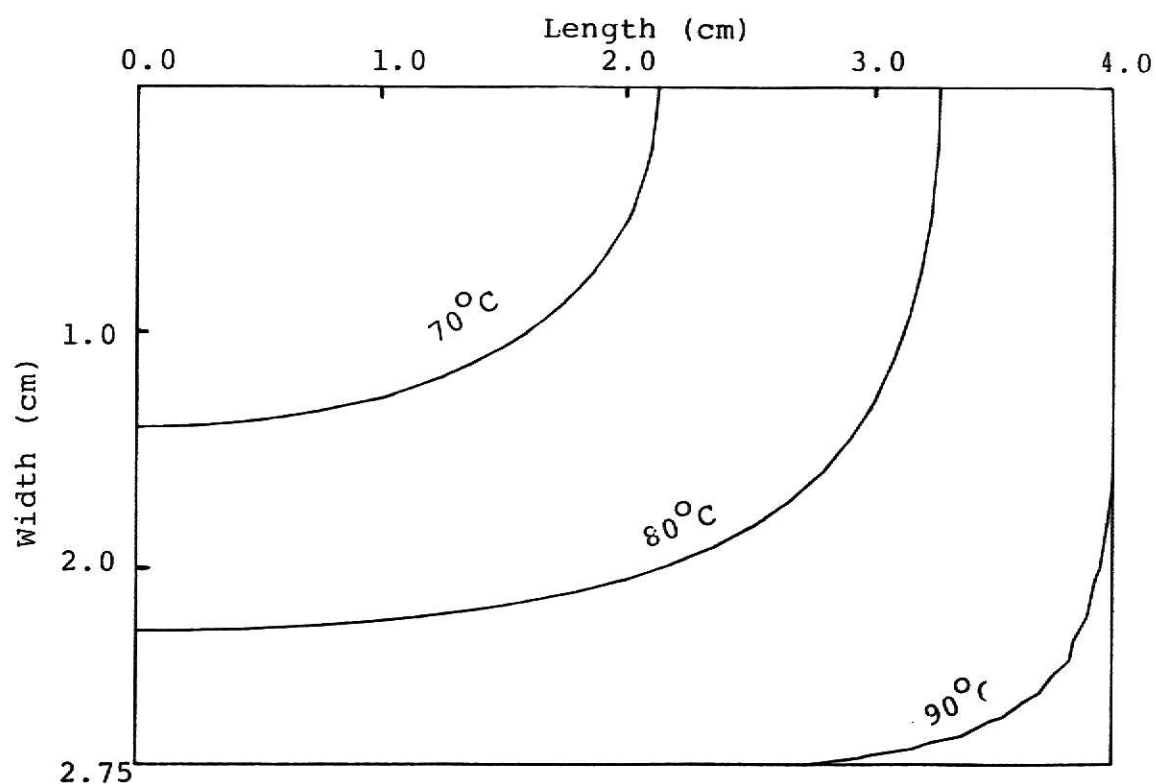
Fig. 3.17.   Simulated temperature profiles for an
oven temperature of 175°C after 60 min.
of cooking.   The origin represents the
center of the meat piece.
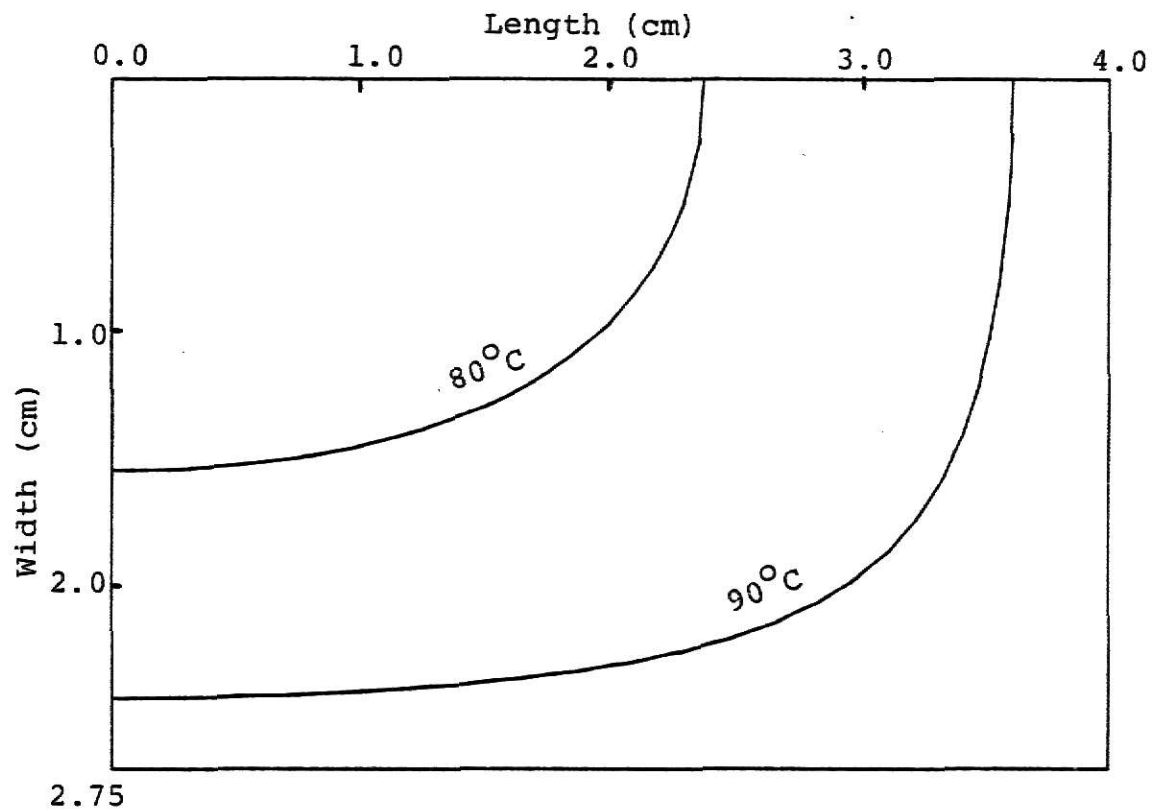
Fig. 3.18. Simulated temperature profiles for an oven temperature of 175°C after 70 min. of cooking. The origin represents the center of the meat piece.

IV. CONCLUSION

### Summary of Results

The mathematical model proposed to describe the roasting
of meat is valid for the constant drying rate period only. In
this period of drying, the surface of the meat remains wet and
the evaporation of moisture from the meat surface can be thought
of as water evaporating from a shallow pool. The constant rate
period of drying (during the roasting of meat) lasts for the
entire heating cycle if the oven temperature is kept low and
the cooking in the oven is done by free convection (low heat
transfer coefficient). Increasing the heat transfer coefficient
and/or the oven temperature eventually causes the surface
temperature to rise and to exceed the wet bulb temperature.
This results in the end of the constant drying rate period
and the start of the falling rate period.

As shown in the previous chapter, moisture loss is an
important factor in the cooking of meat. A major part of the
energy required for cooking is used in evaporating the water
bound in the muscle. Moisture loss is greater when meat is
roasted at higher oven temperatures, but the total cooking
time is reduced. Evaporative losses can be reduced by
raising the relative humidity inside the oven and lowering
the oven temperature. To maintain the same thermal drying

force (same cooking time), the humidity inside the oven can be increased which in effect raises the wet bulb temperature.   Melting of fat is not very critical in modelling the roasting process. As shown earlier, a very small fraction of the energy required for cooking is used for melting the fat contained in the meat.

If the meat is cooked in a closed oven, the humidity and the wet bulb temperature in the oven increase as the cooking.proceed: This happens because the water that evaporates from the meat surface is accumulated in the oven. Since the drying rate and the heat transfer rate are dependent on the humidity and the wet bulb temperature, it is very essential that these changes in the wet bulb temperature and humidity be accounted for in the model describing the roasting process. From the simulation results it was observed that roasting at higher oven temperature results in higher wet bulb temperature, higher surface temperature and steeper temperature gradients. Therefore, it can be concluded that oven temperature, heat transfer coefficient and humidity in the oven have important effects on the cooking of meat.

From the simulation results it can be concluded that the following factors must be considered to model the roasting of meat in the constant drying rate period

1) Convection and conduction heat transfer in meat

2) Evaporation of water from the meat surface

3) Changes in gas phase wet bulb temperature.

On comparing the simulated and experimental results, it was found that the two were in close agreement. For the center temperature to reach 40^OC, the difference in the experimental cooking time and the cooking time obtained from the simulation was less than 3% for both oven temperatures used (T_a = 175°C and 225°C). The difference between the experimental and simulated cooking times was about 12% for the meat to be cooked ' medium ' (center temperature to reach 70°C). As discussed in the previous chapter, this difference is primarily due to the decrease in thermal conductivity of meat due to the evaporation of water from the muscle. The model proposed in this report does not account for the change of thermal conductivity of meat as it cooks. For low center temperatures (below 40°C) the mathematical model gave very accurate results, but it should be modified slightly for higher temperatures.

In modelling the roasting process, the flow of heat was considered only in two dimensions and heat transfer was neglected in the third direction. This was a reasonable assumption since the third dimension of the meat sample used for the experimental results was about three times larger than the other two dimensions. Heat flow in all the three dimensions needs to be considered if the length, width and height of the meat piece are comparable in size.

The Implicit Alternating Direction Method was used to numerically solve the parabolic partial differential equation in two space dimensions. For the sake of mathematical simplicity,

the increment in the x and y directions were taken to be same. As discussed in the first chapter, the Implicit Alternating Direction Method does not impose any restriction on the time increment Δt and the space increment Δx. In the simulations, Δt and Δx were chosen (independent of each other) to be 2.5 min. and 0.25 cm, respectively. This corresponds to a dimensionless time increment $\Delta \tau = 0.035$ and dimensionless space increment $\Delta x = 0.09$. The computer execution time was less than 5.0 sec. Decreasing the time increment by 50%, increases the accuracy of the simulation result by only 0.4%, but increases the computer execution time by about 100%. If the sapce increment Δx is reduced by a factor of 1/2, the simulation time increases by a factor of 4 and the accuracy of the result is improved by about 1°C. It can therefore be concluded that the Implicit Alternating Direction Method is a very efficient scheme to solve the parabolic partial differential equaion in two or more space dimensions. Fairly large values of the space increment and the time increment can be chosen without causing serious errors in the result.

Future Work

The mathematical model proposed in this report for describing the roasting of meat is valid only for the constant drying rate period. If the meat is cooked at a higher oven temperature or if the roasting is done in a forced convection oven, the constant rate period may last for a very short time,

thus limiting the use of this model. In order to make the model
more versatile, it should be extended to describe the falling
rate period of drying also. The falling rate period starts
when the surface temperature exceeds the wet bulb temperature
in the oven. During this stage of drying, the meat surface
is relatively dry and evaporation no longer takes place from
the meat surface. The evaporating zone is moved inside the
meat. Evaporation takes place in the vicinity of the 100°C
isotherm. Transport of water below the 100°C isotherm takes
place by capillary flow of the liquid. Transport of water above the 100°C
isotherm (in the crust) takes place in the vapor phase. Unlike the
constant drying rate period, where the drying rate is con-
trolled by the external conditions, the drying rate in the
falling rate period is controlled by the transport of water
in the meat. The amount of water that is evaporated depends
on the amount of water that is transported to the evaporating
zone. This requires a model which describes the migration of
moisture in the meat.

As stated in the previous paragraph, the evaporation
(in the falling rate period) takes place very close to the
100°C isotherm. As cooking proceeds, the 100°C isotherm
moves further inside the meat and as a result the boundary at
which evaporation takes place no longer remains stationary.
Due to this, the thickness of the crust increases as cooking
progresses. Since the transport of vapor in the crust is
inversely proportional to its thickness, the resistance to
the flow of vapor increases causing the drying rate to decrease.

The thermal conductivity of meat depends on its fat and water content. It is known that the water content of meat decreases markedly as it cooks. Therefore, there is a need to consider the variation of thermal conductivity of meat with moisture content. This requires a model for moisture content as a function of position.

Summarizing the above results, it can be concluded that the following factors need to be considered in modelling the falling rate period.

1) Convection and conduction heat transfer in meat

2) Migration of moisture in meat

3) Evaporation of water near the 100°C isotherm

4) Moving evaporating boundary

5) Variation of thermal conductivity of meat with moisture content.

Measurement of thermal conductivity, density, and specific heat of meat have been made by several researchers [8, 9, 10] and their values can be easily obtained from the literature. So far no work has been reported on the measurement of diffusivity of water in meat ($\beta = \delta/\rho_s$). In order to model the migration of water in meat, it is necessary to estimate the value of the parameter β. Since the flow of water in the crust takes place as vapor, it is also necessary to estimate the value of the mass transfer coefficient k_p in the crust.

V. APPENDIX
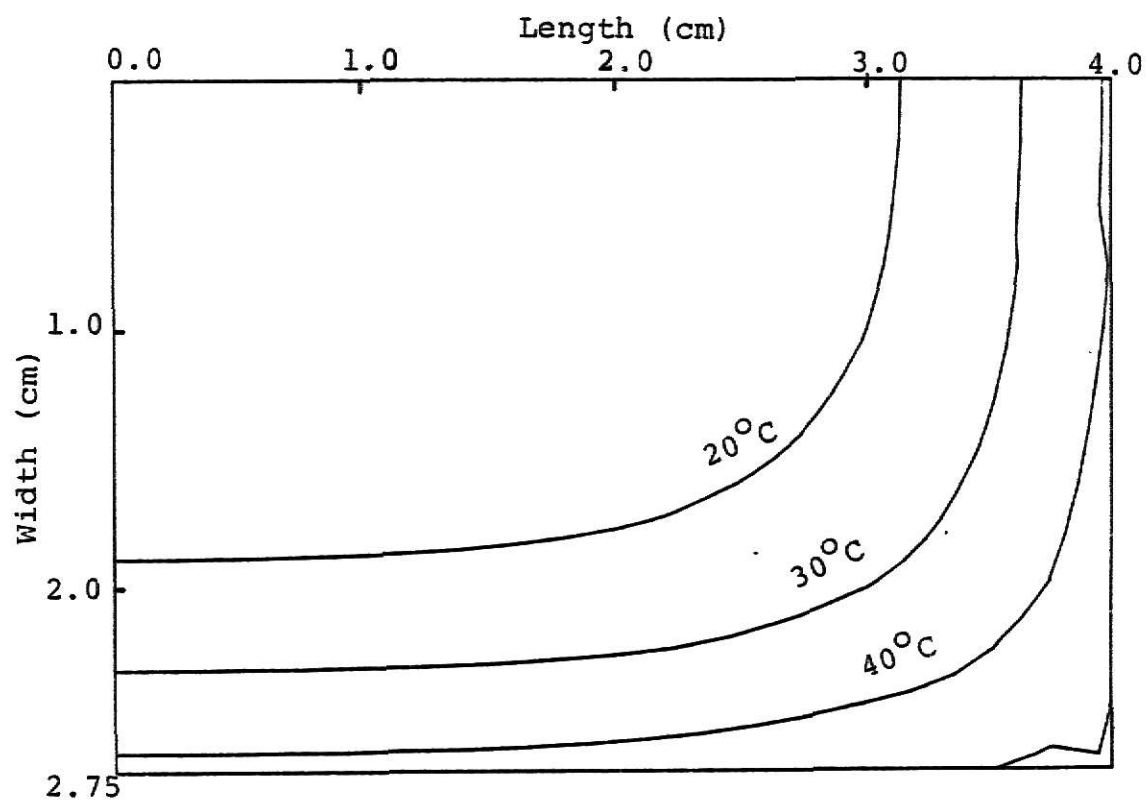
Fig. 5.1.   Simulated temperature profiles for an
oven temperature of 225°C after 10 min.
of cooking.   The origin represents the
center of the meat piece.
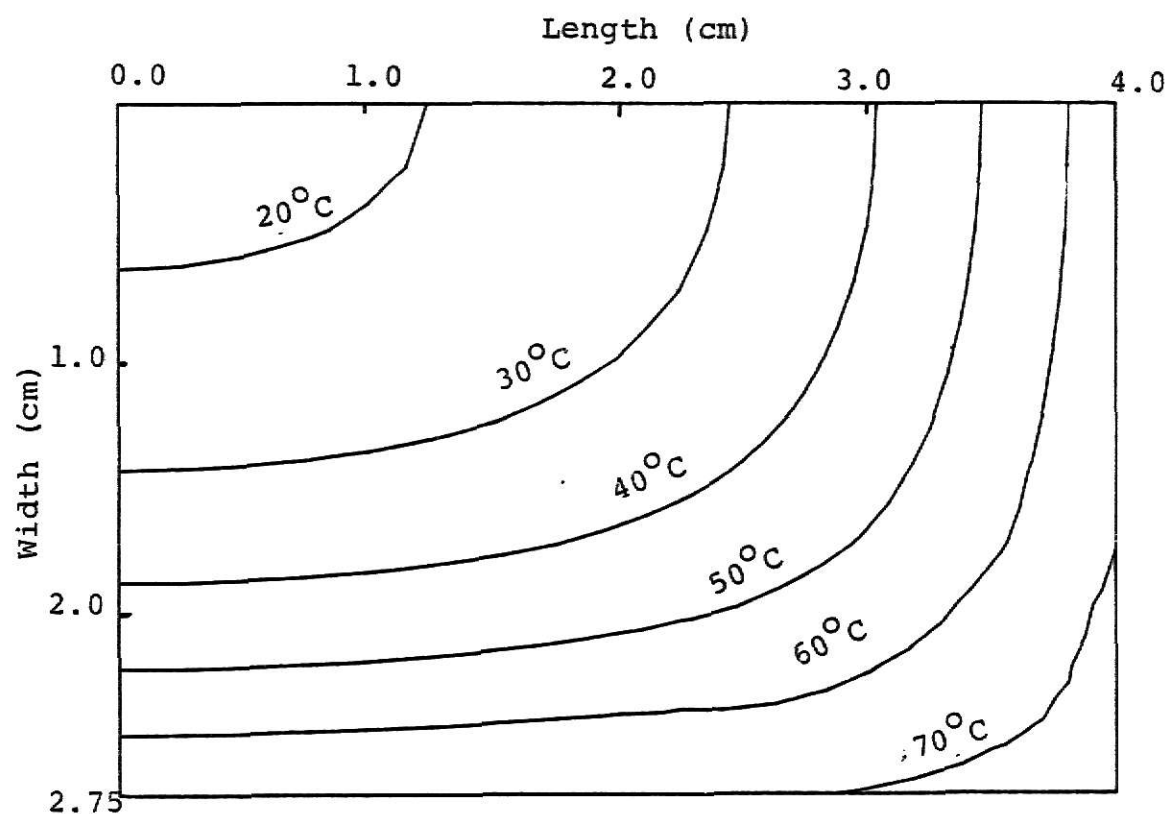
Fig. 5.2.   Simulated temperature profiles for an
oven temperature of 225°C after 20 min.
of cooking.   The origin represents the
center of the meat piece.
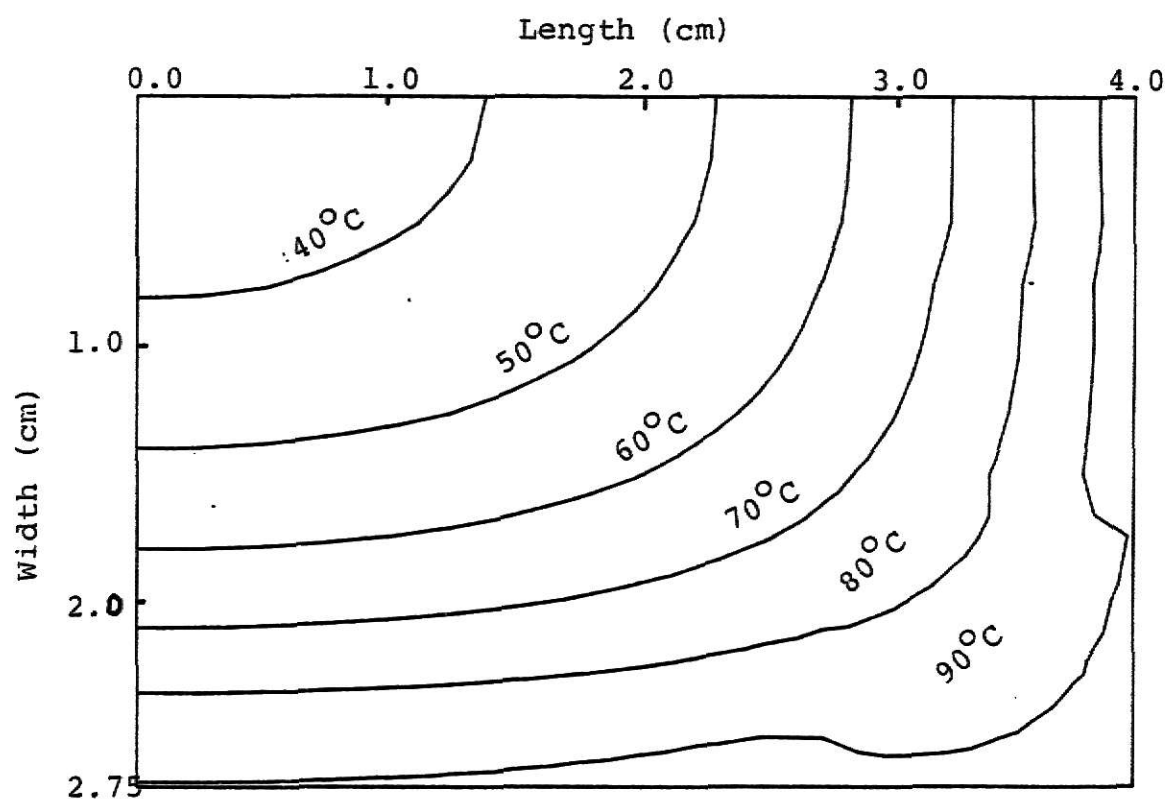
Fig. 5.3. Simulated temperature profiles for an oven temperature of 225°C after 30 min. of cooking. The origin represents the center of the meat piece.
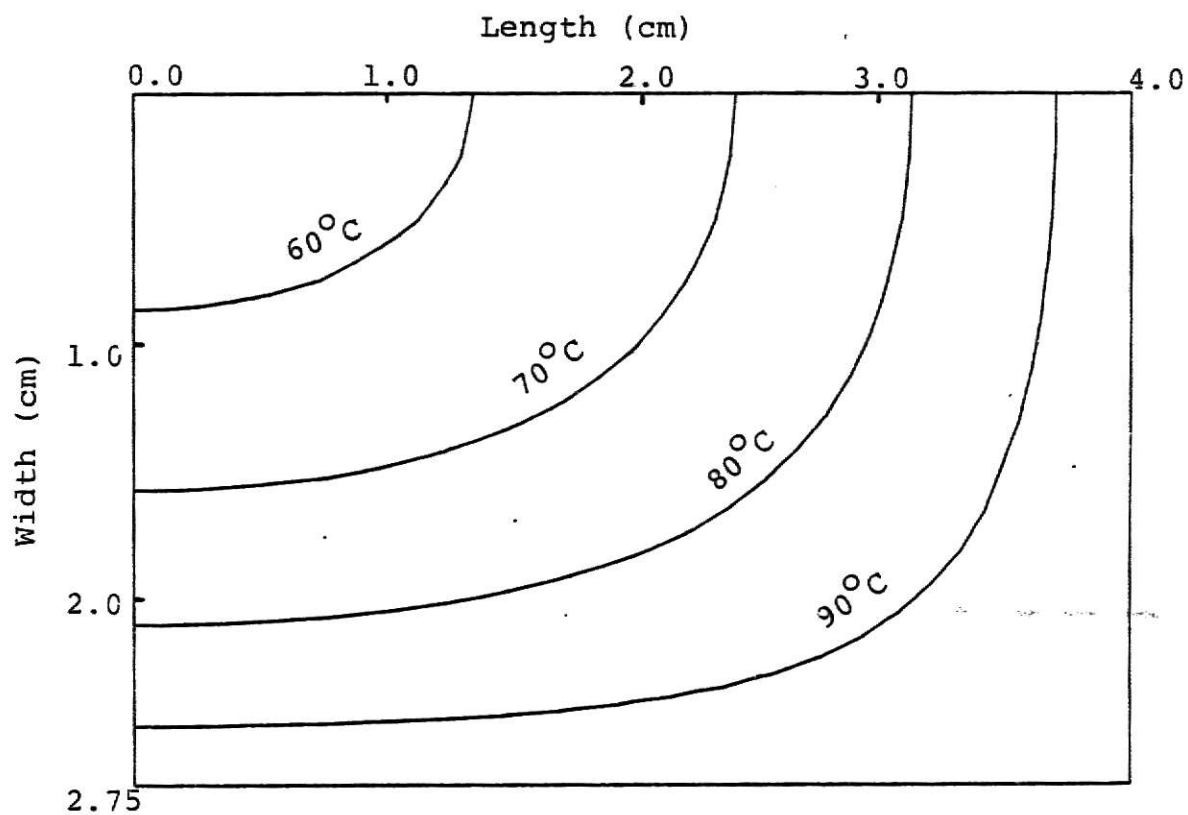
Fig. 5.4. Simulated temperature profiles for an oven temperature of 225°C after 40 min. cooking. The origin represents the center of the meat piece.
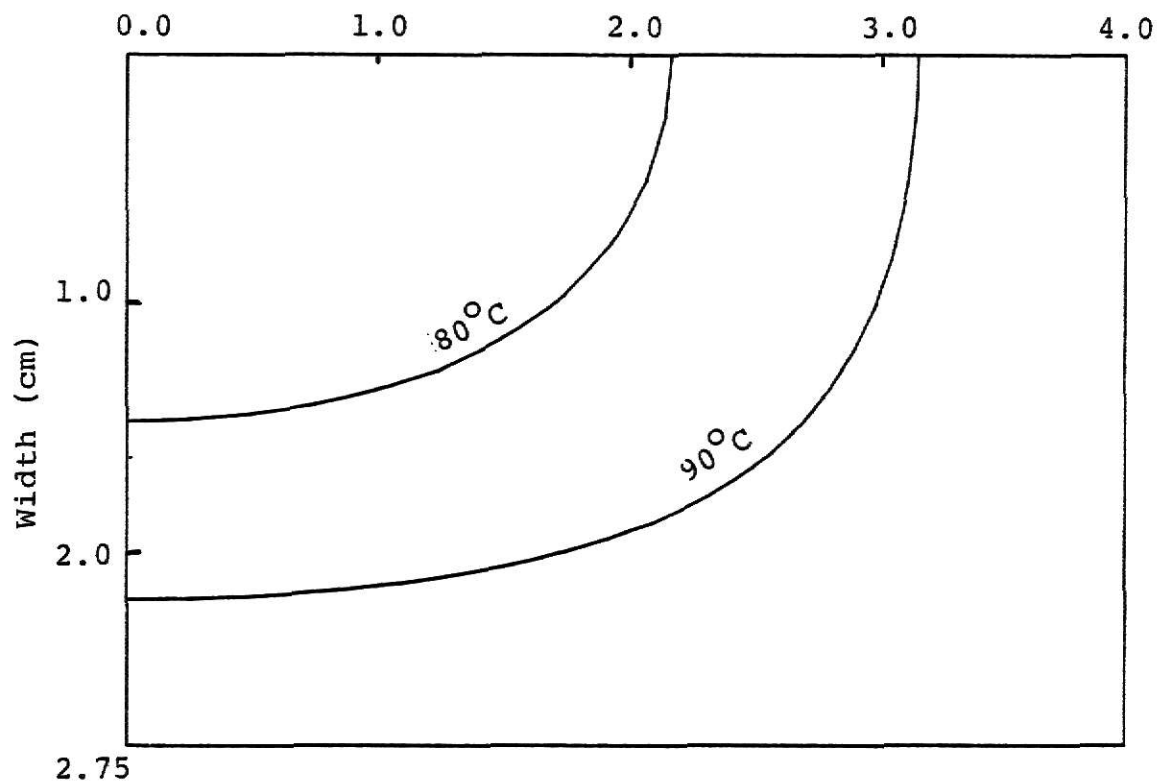
Fig. 5.5.   Simulated temperature profiles for an
oven temperature of 225°C after 50 min.
cooking.   The origin represents the
center of the meat piece.
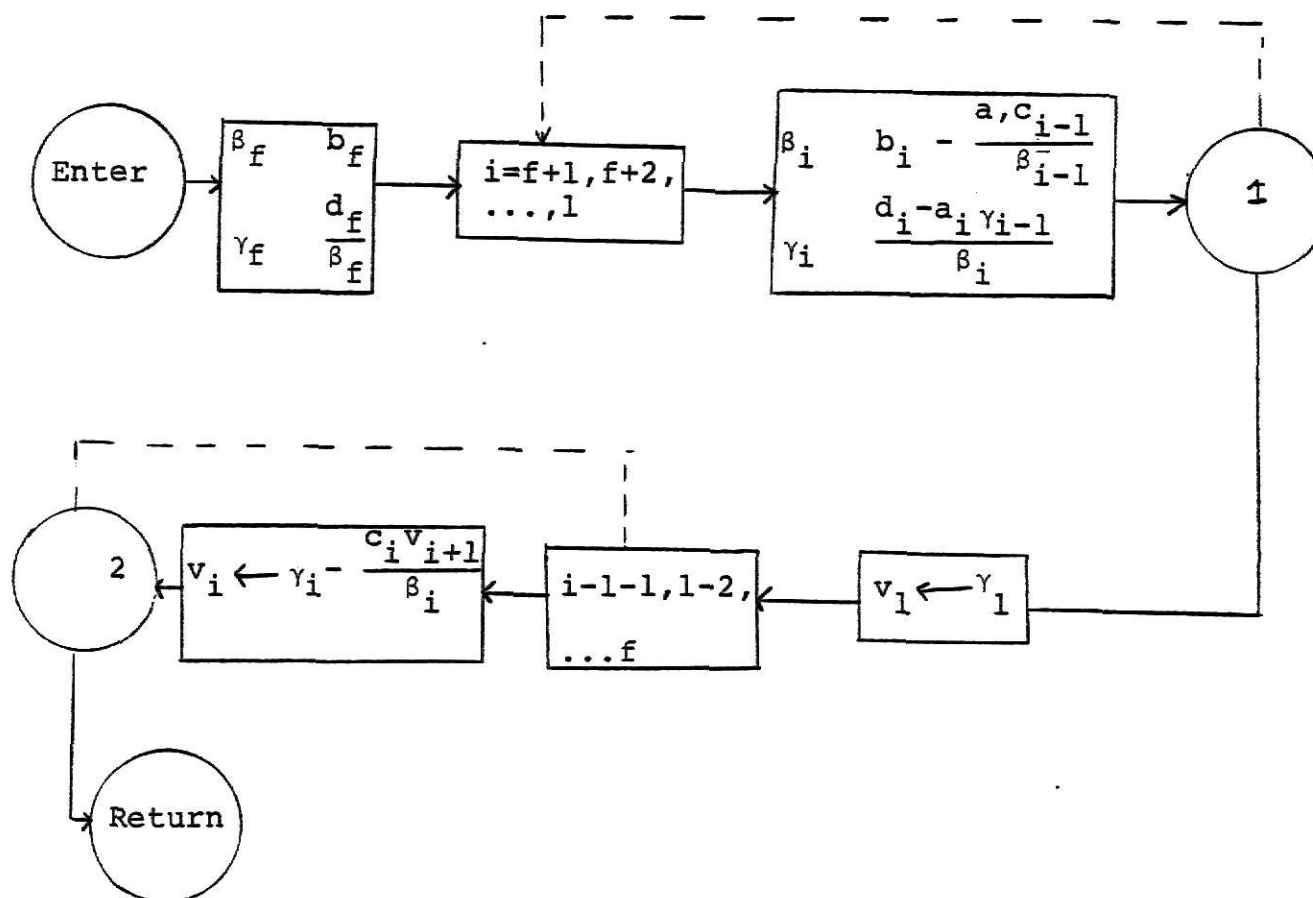
Subroutine TRIDAG (Dummy arguments: f, l, a, b, c, d, v;

calling arguments: l, M-1, a, b, c, d, T)

Fig. 5.6. Subroutine Tridag

Nomenclature

a   = width of the meat piece (m)

a'   = surface Area of the meat (m^2)

A,B   = constants of Equation (2.6) (Pascals and Pascals/^{o}C)

c_p = heat capacity of meat at constant pressure (J/kg^{o}C)

h   = heat transfer coefficient between air and meat
        (J/m^2 sec ^{o}C)

H   = humidity inside the oven (kg of water/kg dry air)

k   = thermal diffusivity in the meat (J/m sec ^{o}C)

k_p = mass transfer coefficient between air and meat (kg/
        m^2 Pascals sec = sec/m)

M_a = mass of air in the oven (kg)

M_t = total moles of air and water vapor in the oven (kg-moles)

M_v = moles of air and water vapor vented from the oven
        (kg/moles)

M_w = moles of water vapor in the oven (kg-moles)

P   = total pressure in the oven (Pascals)

P_a = partial pressure of water vapor in air (Pascals)

P_s = water vapor pressure at the meat surface (Pascals)

t   = time (sec)

T   = dimensionless temperature

T_c = center temperature of the meat piece (^{o}C)

T_w = wet bulb temperature in the oven (^{o}C)

T_s = surface temperature of the meat piece

V   = volume of oven (m^3)

W   = mass of water vapor in the oven (kg)

x, y, z = dimensionless space variable

X, Y, Z = space variables (m)

α = thermal diffusivity in the meat (m^2/sec)

β = water difffusivity in the meat (m^2/sec)

Δx = increment in the x direction (m)

Δy = increment in the y direction (m)

Δt = time increment (sec)

τ = dimensionless time

$\Delta \tau$ = dimensionless time increment

ΔW = mass of water evaporated from the meat in the time interval Δt

λ = latent heat of vaporization of water (J/kg)

ρ = density of meat (kg/m^3)

ρ_a = density of air (kg/m^3)

θ = temperature (^{O}C)

θ_a = ambient temperature (^{O}C)

θ_O = initial temperature of the meat piece (^{O}C)

Subscripts

i = represents position on the x axis

j = represents position on the y axis

k = represents level of time

```
      * * * * * * * * * * * * * * * * * * * * * * * * * * *
C     * THIS PROGRAM SOLVES FOR THE UNSTEADY STATE HEAT      *
C     * CONDUCTION IN A RECTANGULAR MEAT SLAB USING THE I.A.D *
C     * METHOD.  INITIALLY THE TEMPERATURE OF THE MEAT IS    *
C     * UNIFORM EVERYWHERE AND IS EQUAL TO TO.  AT TIME T=0,  *
C     * THE MEAT IS EXPOSED TO HOT AIR IN THE OVEN AT TEMPER- *
C     * ATURE TA.  WATER IS TRANSPORTED FROM THE MEAT SURFACE *
C     * TO THE HOT AIR HEATING THE MEAT.  THE HUMIDITY AND   *
C     * THE WET BULB TEMPERATURE IN THE OVEN CHANGES AS THE   *
C     * MEAT COOKS.                                          *
C     * THE PARAMETERS USED ARE:                             *
C     * K=THERMAL CONDUCTIVITY OF MEAT IN J/(M SEC'C)        *
C     * LAMDA=LATENT HEAT OF VAPORIZATION IN J/KG            *
C     * ALPHA=THERMAL DIFFUSIVITY IN THE MEAT M2/SEC         *
C     * KP=MASS TRANSFER COEFFICIENT IN SEC/M                *
C     * PA=VAPOUR PRESSURE OF AIR IN PASCALS                 *
C     * H=HEAT TRANSFER COEFFICIENT IN J/(M2 SEC'C)          *
C     * TA=AMBIENT TEMPERATURE OF HOT AIR IN 'C              *
C     * TO=INITIAL TEMPERATURE OF MEAT IN 'C                 *
C     * TM=MAX.CENTER TEMP. TO WHICH THE MEAT IS TO BE       *
C     *     HEATED IN 'C                                     *
C     * A1=WIDTH OF THE RECTANGULAR MEAT SLAB IN M           *
C     * B3=LENGTH OF THE RECTANGULAR MEAT SLAB IN M          *
C     * * * * * * * * * * * * * * * * * * * * * * * * * * *
C
      DIMENSION A(50),B(50),C(50),D(50),T(50,50),TSTAR(50,50)
      DIMENSION B1(50),TPRIME(50),THETA(50,50)
      REAL K,KP,LAMDA,MOLE
C
C     READ AND CHECK INPUT PARAMETERS
C
C     N=GRID SIZE
C     M=GRID SIZE
C     DT=TIME INCREMENT IN MINS.
C     DTAU=DIMENSIONLESS TIME INCREMENT
C     AIR=MASS OF AIR IN THE OVEN IN KG
C     MOLE=MOLES OF AIR IN THE OVEN IN KG-MOLE
C     W=MASS OF WATER IN THE OVEN IN KG
C     VAPL=MASS OF WATER THAT HAS VAPORISED IN KG
C
      READ (5,*)TM,A1,B3
      READ(5,*)K,ALPHA,TA,TO
      READ(5,*)N,M
      READ(5,*)DT
      READ(5,*)PA
      READ(5,*)H
      READ(5,*)LAMDA
      DTAU=(ALPHA*60.0*DT)/A1**2
      AIR=0.0137
      MOLE=AIR/29.0
      W=0.
      VAPL=0.
C
      WRITE(6,500)DTAU,N,A1,B3
      WRITE(6,501)ALPHA,H,K,PA
      WRITE(6,502)TA,TO,TM
      WRITE(6,503)
```

```
C
      Z=H/(64.7*K)
      TMAX=(TM-TO)/(TA-TO)
      NP1=N+1
      MP1=M+1
      FLOATN=N
      DX=1/FLOATN
      G1=A1*H*DX/K
      RATIO=DTAU/(DX*DX)
      ICONT=1
C
C     SET INITIAL TEMP. IN THE SLAB
C
      DO 2 I=1,NP1
      DO 2 J=1,MP1
      T(I,J)=0.0
2     TSTAR(I,J)=0.0
C
C     SET COEFFICIENT ARRAYS A,B,C OF THE TRIDAG. MATRIX
C
      B(1)=2.0*(1.0/RATIO+1.0)
      B1(1)=B(1)
      F=2.0*(1.0/RATIO-1.0)
      DO 3 I=2,M
      A(I)=-1.0
      B(I)=B(1)
      B1(I)=B(1)
3     C(I)=-1.0
      C(1)=-2.0
      BN=B(N)
      TAU=0.0
4     TAU=TAU+DTAU
C
C     COMPUTE TEMP. AT THE END OF HALF TIME INCREMENT
C     (IMPLICIT BY ROWS)
C
      DO 8 J=1,M
      DO 7 I=1,N
      IF(J.NE.1)GO TO 6
      D(I)=2.0*T(I,2)+F*T(I,1)
      GO TO 7
6     D(I)=T(I,J-1)+F*T(I,J)+T(I,J+1)
7     CONTINUE
C
C     CALCULATE THE COEFFICIENT A2 & B2 OF ANTOINE'S
C     EQUATION
C     ANTOINE'S EQUATION : PS=A2+B2*THETA
C     FOR TEMP. RANGE 0-30'C,A2=-126.4 PA,B2=140.9 PA/'C
C                     30-50'C,A2=-8357.0 PA,B2=412.2 PA/'C
C                     50-70'C,A2=-36001.8 PA,B2=958.9 PA/'C
C                     70-90'C,A2=-108230.9 PA,B2=1983.7 PA/'C
C
      IF(T(I,J)-0.14706)51,51,52
52    IF(T(I,J)-0.26470)53,53,54
54    IF(T(I,J)-0.38235)55,55,56
51    A2=-126.4
      B2=140.9
```

```
         GO TO 5
53       A2=-8357.0
         B2=412.2
         GO TO 5
55       A2=-36001.8
         B2=958.9
         GO TO 5
56       A2=-109230.0
         B2=1983.7
5        H1=(A2-PA+B2*T0)/(B2*(TA-T0))
         G2=A1*Z*B2*DX
         G=G1+G2
         B(N)=BN-RATIO/(1.0+RATIO*(1.0+G))
C
         IF(J.NE.1)GO TO 16
         E=RATIO*(T(NP1,J+1)-T(NP1,J)+G1-G2*H1)+T(NP1,J)
         GO TO 17
16       E=0.5*RATIO*(T(NP1,J-1)+T(NP1,J+1)-2.0*T(NP1,J)
        1+2.0*(G1-G2*H1))+T(NP1,J)
17       D(N)=D(N)+E/(1.0+RATIO*(1.0+G))
         CALL TRIDAG(1,N,A,B,C,D,TPRIME)
         DO 9 I=1,N
9        TSTAR(I,J)=TPRIME(I)
8        TSTAR(NP1,J)=(RATIO*TSTAR(N,J)+E)/(1.0+RATIO*(1.0+G))
C
C        COMPUTE TEMP. OF THE M+1TH COLUMN AT THE END OF
C        HALF TIME INCREMENT
C
         DO 26 I=1,N
         TSTAR(I,MP1)=(G1-G2*H1+TSTAR(I,M))/(1.0+G)
26       CONTINUE
C
C        COMPUTE CORNER TEMP. AT THE END OF HALF TIME INCREMENT
C
         TSTAR(NP1,MP1)=0.5*(TSTAR(NP1,M)+TSTAR(N,MP1))
C
C        COMPUTE TEMP. AT THE END OF FULL TIME INCREMENT
C
         DO 12 I=1,N
         DO 11 J=1,M
         IF(I.NE.1)GO TO 10
         D(J)=2.0*TSTAR(2,J)+F*TSTAR(I,J)
         GO TO 11
10       D(J)=TSTAR(I-1,J)+F*TSTAR(I,J)+TSTAR(I+1,J)
11       CONTINUE
C
C        COMPUTE ANTOINE'S COEFFICIENT A2  & B2
C
         IF(TSTAR(I,J)-0.14706)61,61,62
62       IF(TSTAR(I,J)-0.26470)63,63,64
64       IF(TSTAR(I,J)-0.38235)65,65,66
61       A2=-126.8
         B2=140.0
         GO TO 15
63       A2=-8357.0
         B2=412.2
         GO TO 15
```

```
65      A2=-36001.8
        B2=958.9
        GO TO 15
66      A2=-108230.0
        B2=1983.7
15      H1=(A2-PA+B2*TO)/(B2*(TA-TO))
        G2=A1*Z*B2*DX
        G=G1+G2
        B1(M)=BN-RATIO/(1.0+RATIO*(1.0+G))
C
        IF(I.NE.1)GO TO 21
        E1=RATIO*(TSTAR(I+1,MP1)-TSTAR(I,MP1)+G1-G2*H1)
     1+TSTAR(I,MP1)
        GO TO 22
21      E1=0.5*RATIO*(TSTAR(I-1,MP1)+TSTAR(I+1,MP1)
     1-2.0*TSTAR(I,MP1)+2.0*(G1-G2*H1))+TSTAR(I,MP1)
22      D(M)=D(M)+E1/(1.0+RATIO*(1.0+G))
        CALL TRIDAG(1,M,A,B1,C,D,TPRIME)
        DO 23 J=1,M
23      T(I,J)=TPRIME(J)
12      T(I,MP1)=(RATIO*T(I,M)+E1)/(1.0+RATIO*(1.0+G))
C
C       COMPUTE TEMP. OF N+1TH ROW AT THE END OF FULL TIME
C       INCREMENT
C
        DO 27 J=1,M
        T(NP1,J)=(G1-G2*H1+T(N,J))/(1.0+G)
27      CONTINUE
C
C       COMPUTE CORNER TEMP. AT THE END OF FULL TIME INCREMENT
C
        T(NP1,MP1)=0.5*(T(NP1,M)+T(N,MP1))
C
        TIME=TAU*A1**2/(ALPHA*60.0)
        DO 50 I=1,NP1
        DO 50 J=1,MP1
50      THETA(I,J)=T(I,J)*(TA-TO)+TO
C       **************************************************************
C
C
C       COMPUTE ANTOINE'S COEFFICIENT A2 &B2
C
        IF(THETA(NP1,MP1)-30.0)71,71,72
72      IF(THETA(NP1,MP1)-50.0)73,73,74
74      IF(THETA(NP1,MP1)-70.0)75,75,76
71      A2=-126.4
        B2=140.9
        GO TO 77
73      A2=-8357.0
        B2=412.21
        GO TO 77
75      A2=-36001.8
        B2=958.89
        GO TO 77
76      A2=-108230.9
        B2=1983.7
C
C       COMPUTE VAPOUR PRESSURE OF WATER AT THE SURFACE
```

```
C
77      PS=A2+B2*THETA(NP1,MP1)
C
C       COMPUTE AMT. OF MOISTURE LOST
C
        KP=H/(64.7*LAMDA)
        AREA=.15*2.0*(.055+.08)+2.0*.055*.08
        WPR=KP*(PS-PA)*2.5*60.0*AREA
        VAPL=VAPL+WPR
        W=KP*(PS-PA)*AREA*DT*60.0+W
        WMOLE=W/18.0
        AMOLE=AIR/29.0    .
        TMOLE=AMCLE+WMOLE
        VMOLE=TMOLE-MOLE
        VAIR=AMOLE*VMOLE*29.0/TMOLE
        VW=WMOLE*VMOLE*18.0/TMOLE
        AIP=AIR-VAIR
        W=W-VW
        HUM=W/AIR
        PA=HUM*29.0*103225.0/(18.0+HUM*29.0)
        VOL=PA*100.0/103225.0
        TW=(PA/0.0002418)**(1/4.33333)
        IF(ICONT.EQ.4)GO TO 998
        GO TO 999
998     WRITE(6,201)TIME
        WRITE(6,204)VAPL,PA,VOL,TW
        DO 14 I=1,NP1
        WRITE(6,202)(THETA(I,J),J=1,MP1)
C       WRITE(6,203)
14      CONTINUE
999     ICONT=ICONT+1
        IF(ICONT.EQ.5)ICONT=1
100     IF(T(1,1)-TMAX)4,4,1
201     FORMAT(/,' AT A TIME T = ',F8.2,/)
202     FORMAT(17F7.2)
C203     FORMAT('                  ')
204     FORMAT(' MS=',F8.6,/,' PA=',F9.2,/,' VOL%=',F5.2,/,
       1' TW=',F6.2,/)
500     FORMAT(' THE INPUT PARAMETERS ARE  :',/,/,' DTAU  = ',
       1F4.2,/,' N      = ',I2,/,' A1    = ',F6.4,/,' B3    = '
       1,F6.4)
502     FORMAT(' TA    = ',F5.1,/,' TO   = ',F4.1,/,' TM    =
       1 ',F4.1)
501     FORMAT(' ALPHA = ',F11.9,/,' H     = ',F5.2,/,' K
       1= ',F4.2,/,' PA    = ',F8.2)
503     FORMAT(' ************************************************')
1       STOP
        END
C
C       ************************************************************
        SUBROUTINE TRIDAG(IF,L,A,B,C,D,V)
C       ************************************************************
        DIMENSION A(1),B(1),C(1),D(1),V(1),BETA(101),GAMMA(101)
        BETA(IF)=B(IF)
        GAMMA(IF)=D(IF)/BETA(IF)
        IFP1=IF+1
        DO 1 I=IFP1,L
```

```
      BETA(I)=B(I)-A(I)*C(I-1)/BETA(I-1)
1     GAMMA(I)=(D(I)-A(I)*GAMMA(I-1))/BETA(I)
      V(L)=GAMMA(L)
      LAST=L-IF
      DO 2 K=1,LAST
      I=L-K
2     V(I)=GAMMA(I)-C(I)*V(I+1)/BETA(I)
      RETURN
      END
$ENTRY
72.0 0.0275 0.04
0.4 0.000000180 175.0 5.0
11 16
2.50
0.
5.0
2436000.0
/*
```

REFERENCES

1. R. B. Keey, Drying: Principles and Practice, Pergamon Press (1972).

2. E. W. Godsalve, E. A. Davis and J. Gordon, Water loss rates and temperature profiles of dry cooked bovine muscle, Journal of Food Science, 42, 1038 (1977).

3. E. W. Gosdalve, E. A. Davis and J. Gordon, Effect of oven condition and sample treatment on water loss of dry cooked bovine muscle, J. of Food Science, 42, 1325 (1977).

4. C. Skjoldebrand and B. Hallstrom, Convection Oven Frying: Heat and Mass transport in the product, Journal of Food Science, 45, 1347 (1980).

5. C. Skjoldebrand, Convection oven Frying: Heat and Mass Transfer between air and product, Journal of Food Science, 45, 1354 (1980).

6. N. E. Bengtsson, B. Jakobsson and M. Dagerskog, Cooking of beef by oven roasting: A study of heat and mass transfer, Journal of Food Science, 41, 1047, (1976).

7. J. J. Bimbenet, M. Loncin and H. Brusset, Heat and mass transfer during air drying of solids, The Canadian Journal of Chemical Engineering, 49, 800 (1971).

8. J. E. Hill, J. D. Leitman and J. E. Sunderland, Thermal conductivity of various meats, Food Technology, 21, 1143 (1967).

9. M. S. G. Khandan and M. R. Okos, Effect of cooking on the thermal conductivity of whole and ground lean beef, Journal of Food Science, 46, 1302 (1981).

10. S. L. Polley, O. P. Snyder and P. Kotnoui, A. Computation of thermal properties of food, Food Technology, 36, 76 (1980).

11. R. W. Mandigo and T. J. Janssen, Energy-efficient cooking system for muscle foods, Food Technology, 36, 128 (1982).

12. E. E. Woodams and J. E. Nowrey, Food Technology, 22, 494 (1968).

13. C. P. Lentz, Thermal conductivity of meats, fats, gelatin gels, and ice, Food Technology, 15, 243. (1960).

14. E. B. Stuart and A. Closset, Pore size effect in the freeze drying process, Journal of Food Science, 36, 388 (1971).

15. R. Hamm, Biochemistry of meat hydration, Advances in Food Research, 10, 355 (1960).

16. P. E. Bouton, P. V. Harris and W. R. Shorthose, Effect of ultimate pH upon the water holding capacity and tenderness of mutton, J. of Food Science, 36, 435 (1971).

17. P. E. Bouton, P. V. Harris, and W. R. Shorthose, The effect of ultimate pH on bovine muscle: water holding capacity J. of Food Science, 37, 351 (1971).

18. G. C. Hung, E. H. Davis, J. Gordon and H. T. Davies, Mechanisms of water loss of bovine semitenderous muscles dry cooked from the frozen state, J. Food Science, 43, 1191 (1978).

19. R. Hamm, F. E. Deatherage, Changes in hydration, solubility and changes of muscle protein during heating of meat, Food Research, 25, 587 (1900).

20. E. Laakkonen, G. H. Wellington, J. W. Sheiben. Low temperature, long time heating of bovine muscle. Changes in tenderness water binding capacity, pH and amount of water soluble components, J. of Food Science, 35, 175 (1970).

21. Von Rosenberg, Modern analytic and computational methods in science and mathematics, American Elsevier Publishing Company, Inc., N.Y. 1969.

22. K. Funk, M. A. Boyle, Beef cooking rates and losses, J. of American Dietic Association, 61, 404 (1972).

23. R. B. Bird, W. E. Stewart and E. N. Lightfoot, Transport phenomena, Wiley (1960).

24. L. J. Moore, D. L. Harrison, and A. D. Dayton, Differences among top round steaks cooked by dry or moist heat in a conventional or a microwave oven. J. of Food Science, 45, 777 (1980).

25. H. H. Voris, F. O. Duyne, Low voltage microwave cooking of top round roasts: Energy consumption, thiamen content and palatability. J. of Food Science, 44, 1447 (1979).

26. B. M. Korschgen, R. E. Baldwin, Moist-heat microwave and conventional cooking of round roasts of beef, J. of Microwave Power, 13, 257 (1978).

27. B. Carnahan, H. A. Luther, J. O. Wilkes, Applied Numerical Method, Wiley, (1969).

28. J. H. Perry, C. H. Chilton, Chemical Engineers' handbook, McGraw-Hill (1973).

ACKNOWLEDGMENTS

I have great preasure in expressing my deep gratitude to my advisors, Dr. Larry E. Erickson and Dr. Richard C. Akins, for their help and guidance throughout this work. I would also like to thank Dr. Melvin C. Hunt for his helpful comments and reading of this thesis. I would like to thank my husband Dr. Rajendra Singh for his constant support and encouragement. Appreciation is also extended to Ms. Margit McCabe for her excellent work in typing of this report.

MODELLING AND SIMULATION OF UNSTEADY STATE HEAT AND

MASS TRANSFER IN THE ROASTING OF MEAT

by

NEERA SINGH

B. Tech., Indian Institute of Technology,

Kanpur, 1981

AN ABSTRACT OF A MASTER'S REPORT

submitted in partial fulfillment of the

requirement for the degree

MASTER OF SCIENCE

Department of Chemical Engineering

KANSAS STATE UNIVERSITY

Manhattan, Kansas

1983

ABSTRACT

The purpose of this work was to develop a mathematical model and carry out numerical simulations to describe the process of roasting of meat. Simultaneous heat and mass transfer was considered and the effects of ambient temperature, humidity and heat transfer coefficient on the roasting process were investigated in detail. The results of the mathematical simulations were compared with the existing experimental data and they were found to be in close agreement. The simulations showed that evaporation of water from the meat surface is an important factor in the cooking of meat, whereas the melting of fat is not very critical in the modelling of the roasting process.